NEA/NSC/DOC(92)5
INDC(Ger)-036/L
KfK 5079

PROGRESS REPORT ON NUCLEAR DATA RESEARCH IN THE FEDERAL REPUBLIC OF GERMANY

for the Period April 1, 1991 to March 31, 1992

July 1992

Edited by
S. Cierjacks
Kernforschungszentrum Karlsruhe
Institut für Materialforschung
Federal Republic of Germany

NEA/NSC/DOC(92)5
INDC(Ger)-036/L
KfK 5079

PROGRESS REPORT ON NUCLEAR DATA RESEARCH IN THE FEDERAL REPUBLIC OF GERMANY

for the Period April 1, 1991 to March 31, 1992

July 1992

Edited by
S. Cierjacks
Kernforschungszentrum Karlsruhe
Institut für Materialforschung
Federal Republic of Germany

PREFACE

This report has been prepared to promote the exchange of nuclear data research information between the Federal Republic of Germany and other member states of OECD/NEA and IAEA. It covers progress reports from KfK Karlsruhe, KFA Jülich, the Research Centre Rossendorf, the universities of Dresden, Hannover, Köln, Marburg, as well as from PTB Braunschweig and FIZ Karlsruhe. In this year the progress report appears for the first time under the auspices of the newly established NEA Nuclear Science Committee. The emphasis of the work reported here is on measurement, compilation and evaluation of nuclear data for pure and applied science programs, such as those relevant to fission- and fusion-reactor technology, waste management, accelerator technology, astrophysics research, cosmogenic and meteoritic investigations, production of medically important radioisotopes etc.

Each contribution is presented under the laboratory heading where the work was done. When the work is relevant to requests in the World Request List for Nuclear Data, WRENDA 87/88 (INDC(SEC)-095/URSF), the corresponding request identification numbers are given in the headings of the respective laboratory reports.

Karlsruhe, July 1992 S. Cierjacks

CONTENTS

Page

INSTITUT FÜR SICHERHEITSFORSCHUNG
FORSCHUNGSZENTRUM ROSSENDORF

INSTITUT FÜR KERN- UND ATOMPHYSIK
TECHNISCHE UNIVERSITÄT DRESDEN

Page

KERNFORSCHUNGSZENTRUM KARLSRUHE
INSTITUT FÜR KERNPHYSIK III

1. THE s-PROCESS BETWEEN A = 120 AND 124 : SIGNATURE OF THE NEUTRON DENSITY IN RED GIANTS

W. SCHANZ, F. KÄPPELER, K. WISSHAK, G. REFFO*

The mass region between tin and tellurium is of relevance for s-process nucleosynthesis, since the s-only isotopes ^{122}Te, ^{123}Te, and ^{124}Te provide for a sensitive test of the neutron density during helium burning in Red Giant stars. The neutron capture flow through this region is sketched in fig.1. Provided that the neutron density at the stellar site is low enough, the s-process reaction chain arriving at ^{120}Sn will completely follow the route via ^{121}Sb to ^{122}Te as indicated by the thick lines. In that case, the "local approximation" predicted by the classical approach to yield for neighboring nuclei

$$\sigma N = \text{const.}$$

can sensitively be tested at the example of the three s-only nuclei ^{122}Te, ^{123}Te, and ^{124}Te, which are shielded against the r-process by their stable isobars in Sn and Sb.

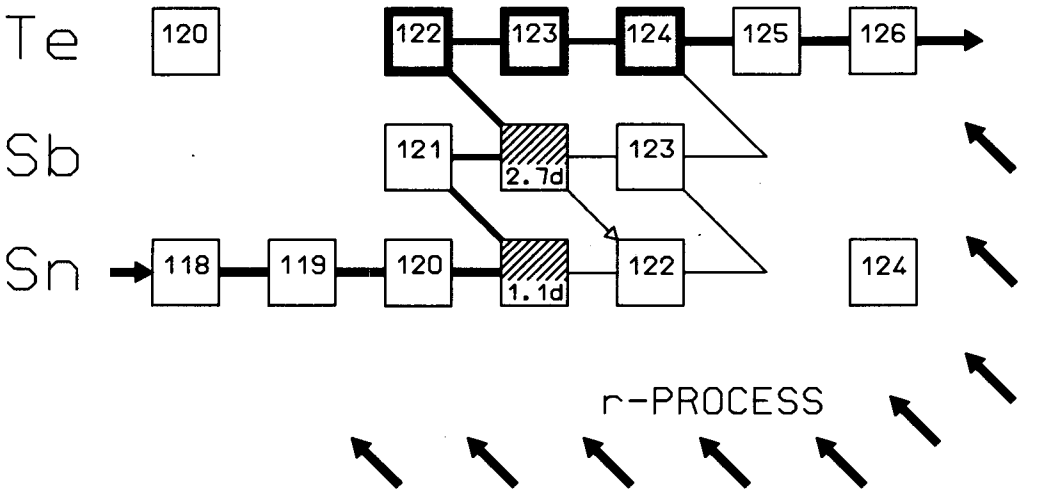

Fig.1 : The s-process neutron capture flow in the mass region 118 < A < 126.

This relation is the consequence of the fact that the s-process abundances are inversely proportional to the stellar (n,γ) cross sections of the respective isotopes. Since the isotopic abundance ratio within a given element is well defined - to better than 0.1% in case of tellurium - the experimental cross section ratios are the decisive quantities for that test. Recent experiments have led to an enormous improvement of these ratios which are known to ±1.2% by now [1]. The reduced uncertainties did not only allow for an impressive confirmation of the local approximation predicted by the classical approach, but indicated also the possibility for identifying a small p-process contribution to the observed ^{122}Te abundance. This feature is important for a quantitative discussion of the p-process, which so far could only be characterized by the neutron-deficient p-only nuclei such as ^{120}Te. In contrast to their compatibility with the classical approach, the new tellurium cross sections gave rise to inconsistencies in the frame of current stellar s-process models, which may bear interesting consequences.

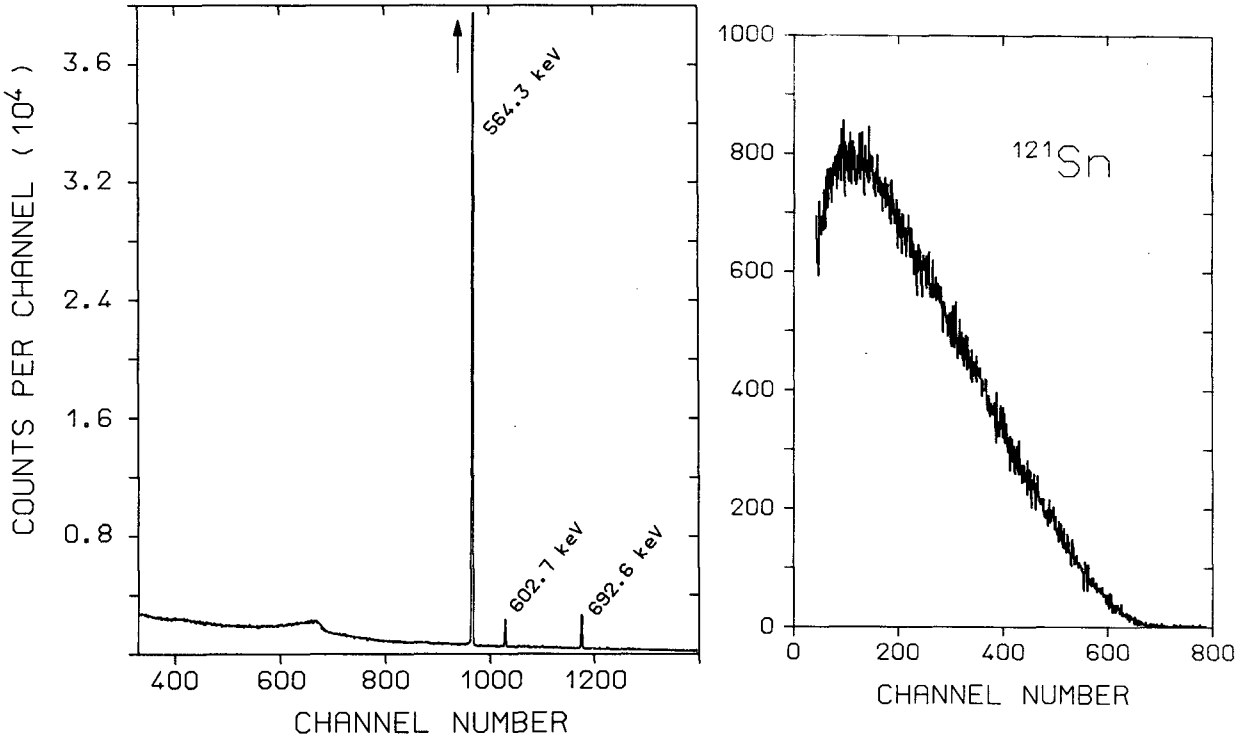

Fig.2: Typical spectra taken from the activated samples. *Left* : A γ-ray spectrum taken from a Sb sample of natural composition, showing the lines associated with the decay of ^{122}Sb (564.3 keV) and of ^{124}Sb (602.7 keV). *Right*: The electron spectrum of an activated ^{120}Sn sample.

In addition to the very accurate cross sections that are available for these s-only nuclei, complementary measurements are reported on ^{120}Sn, ^{121}Sb, ^{123}Sb, and ^{128}Te for an improved analysis of the s-process flow. The measurements were

carried out via the activation technique in a quasi-stellar neutron spectrum for kT=25 keV, using gold as a cross section standard. In case of the antimony cross sections the induced activities could be determined via well known γ-ray transitions in the decay of the respective product nuclei by means of a calibrated HPGe detector. For ^{120}Sn and ^{128}Te such γ-transitions were either missing or unreliable. Therefore, the activities were determined by counting the β-decay electrons directly with a spectrometer consisting of two Si(Li) detectors in close geometry. The 97% efficiency of that spectrometer compensated for the fact that thin samples had to be used with this set-up in order to avoid sizable self-absorption corrections. Fig.2 shows examples for the spectra taken with the two detection methods. In order to study the systematic uncertainties in the present measurements, a whole series of activations was carried out with modified experimental parameters.

The cross sections of the unstable isotopes, ^{121}Sn and ^{122}Sb, were determined by statistical model calculations. The reliability of these results were considerably improved compared to previous calculations by establishing a consistent systematics for the relevant model parameters for all stable nuclei in the mass range of interest. The parameters for the unstable branch points were then inferred from this systematics by interpolation. Uncertainties of $<4\%$ and $<30\%$ were obtained for the measured and calculated results, respectively. Based on these data, s-process analyses are presently be carried out by means of the classical approach and with a stellar model for low mass stars.

[1] K. Wisshak, F. Voss, F. Käppeler, G. Reffo, Report KfK 4899 (1991), Kernforschungszentrum Karlsruhe; Phys. Rev. C (in press)

* ENEA, Laboratorio Dati Nucleari, Bologna Italy

2. AN ADC SYSTEM FOR MEASUREMENTS WITH THE KARLSRUHE 4π BaF_2 DETECTOR

K. GUBER, K. WISSHAK

An ADC system has been added to the electronic equipment of the Karlsruhe 4π Barium Fluoride Detector [1]. It allows to store for each event the gamma-ray energy and time-of-flight (TOF) information of the individual detector modules. A special preprocessing unit rejects events in selectable sum energy and TOF regions. The decision whether an event is accepted is made within 4μs. The system is based on CAMAC modules of type FERA (Le Croy). The hardware trigger is realised by a combination of ALU- (arithmetic logic unit) and MLU- (multiplicity logic unit) modules. Accepted events are transmitted from a data stack to a set of two memorys that are mutually used for input and output. The ADC-system in conjunction with the preprocessing is able to accept a count rate up to 60 kHz.

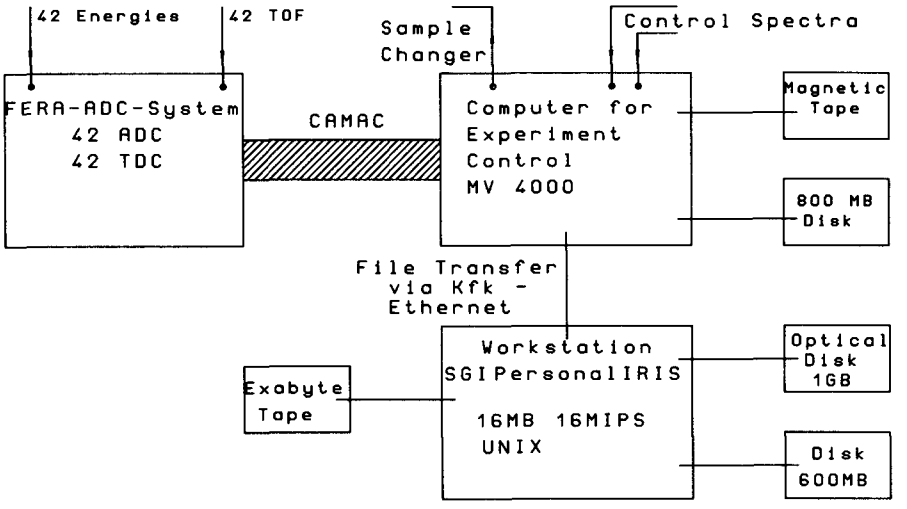

Fig. 1 : Schematic view of the data acquisition of the Karlsruhe 4π BaF_2 detector using an ADC system.

The purpose of the ADC system is : (i) to measure capture gamma-ray spectra, necessary to determine the detector efficiency for capture events, which are presently taken from theoretical calculations [2], (ii) to allow for a deeper understanding of the capture process, e.g. by determining angular or multiplicity distributions of capture gamma-rays, (iii) to reduce significantly the recorded event rate by rejecting those events that are not needed for the evaluation of the cross section e.g. low sum energies and large TOFs, (iv) to improve the resolution in gamma-ray sum energy by off-line correction of the nonlinearity of the individual detector modules.

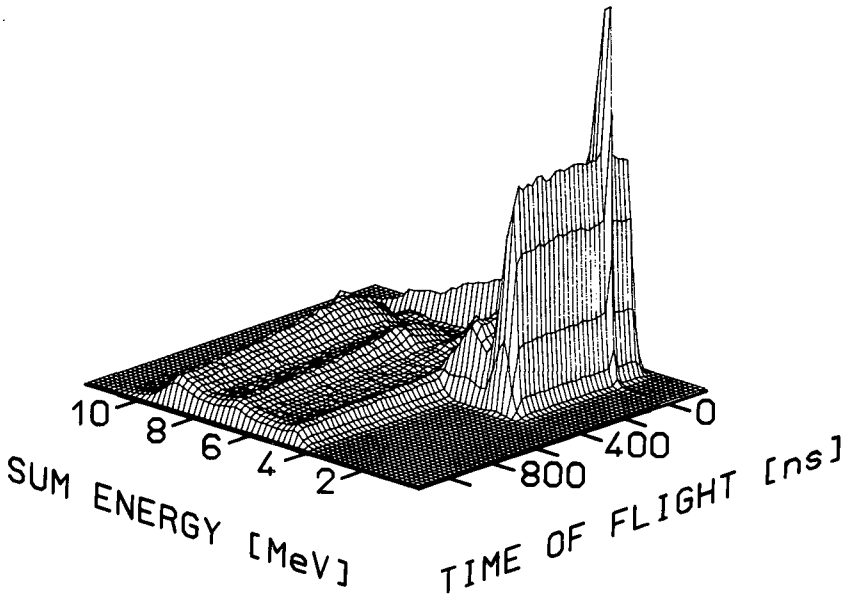

Fig. 2 : Two-dimensional sum energy versus TOF spectrum as calculated from the events recorded with the ADC system. About 50% of the countrate located at low sum energy and large TOF are suppressed by the hardware trigger.

The data acquisition is schematically shown in fig.1. The events from one sample are stored on-line as a diskfile using a MV 4000 computer. After an acquisition time of ~10 min, while the data of the next sample are recorded, the file is transferred via Ethernet to a Silicon Graphics workstation where they are finally stored either on optical disk or on an Exabyte tape. The workstation is lateron used to sort the individual events into two-dimensional sum energy versus TOF spectra dependent on detector multiplicity. An example of such a spectrum is shown in fig.2. Background events at low sum energy and large TOF are completely suppressed by the hardware trigger. The sorting procedure on the workstation is faster by a factor of 18 compared to the respective step of data evaluation on the MV 4000 computer used in previous experiments [2].

The ADC system was used in a first experiment on samarium isotopes. The evaluated cross sections agreed with the respective data measured with the old acquisition system [2] well within the statistical uncertainties.

[1] K. Wisshak, K. Guber, F. Käppeler, J. Krisch, H. Müller, G. Rupp, F. Voß, Nucl. Instr. Meth. **A292**, (1990) 595

[2] K. Wisshak, F. Voß, F. Käppeler, G. Reffo, Phys. Rev. **C42** (1990) 1731

3. NEUTRON CAPTURE IN ^{148,150}Sm : A SENSITIVE PROBE OF THE s-PROCESS NEUTRON DENSITY

K. GUBER, K. WISSHAK, F. KÄPPELER, F. VOß

The neutron capture cross sections of ^{147,148,149,150,152}Sm have been measured in the energy range from 3 to 225 keV at the Karlsruhe Van de Graaff accelerator

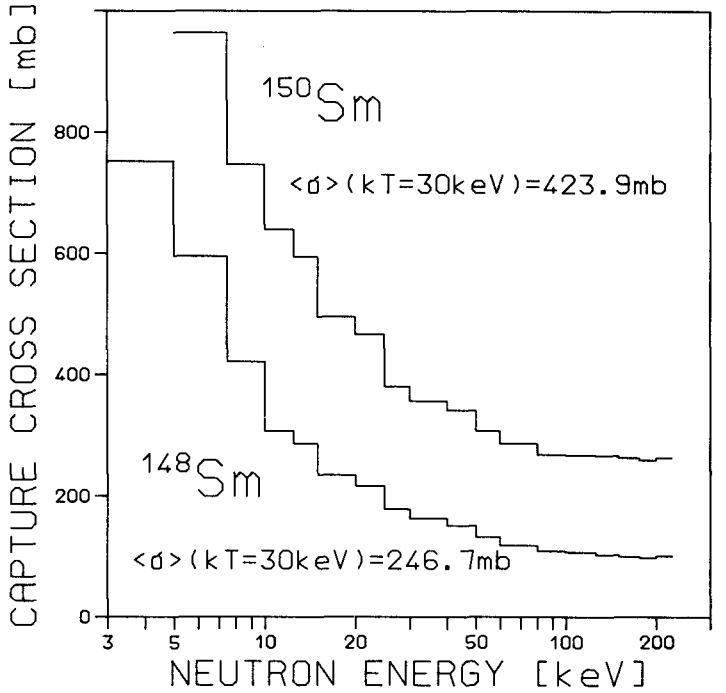

Fig.1 : The neutron capture cross section of the two s-only isotopes ^{148,150}Sm in the energy range from 3 to 225 keV (preliminary values).

using gold as a standard. Neutrons were produced via the ^{7}Li(p,n)^{7}Be reaction by bombarding metallic Li targets with a pulsed proton beam. Capture events were registered with the Karlsruhe 4π Barium Fluoride Detector. Several sets of measurements have been performed under different experimental conditions to study the systematic uncertainties in detail. For the first time, in one of the measurements an ADC system was used for data acquisition that registers separately gamma-ray energy and time-of-flight of all detector modules. The cross section ratios σ(Sm)/σ(Au) were determined with an overall uncertainty of ~1%. This is an improvement by a factor 4 compared to the best experiment performed so far [1]. A preliminary result for the capture cross sections of the two s-only isotopes ^{148,150}Sm is shown in fig.1.

Maxwellian averaged neutron capture cross sections were calculated for thermal energies between kT=10 and 100 keV. In the energy range not covered by the present experiment, resonance parameters from literature and model

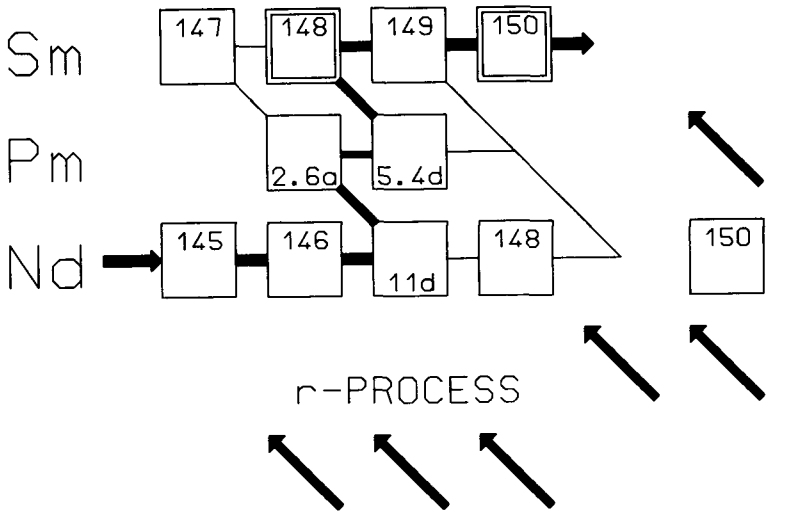

Fig.2 : The s-process path in the region of the samarium isotopes.

calculations were used. As a preliminary result, the ratio of s-process abundance N_S times stellar cross section $<\sigma>$ of ^{148}Sm and ^{150}Sm, was determined (kT=30 keV) :

$$R = N_S <\sigma> (^{148}Sm) / N_S <\sigma> (^{150}Sm) = 0.887 \pm 0.008.$$

This result is in agreement with the number quoted in ref. 1, but the uncertainty has been improved by a factor 4. The deviation of R from unity indicates that the "local approximation" of the s-process ($N_S <\sigma> =$const.), which was well established for the tellurium isotopes [2] is violated in case of samarium due to a significant branching of the s-process path at the unstable isotopes ^{147}Nd, ^{147}Pm and ^{148}Pm (see fig.2). This branching is very sensitive to the s-process neutron density n_n. A first analysis in the framework of the classical model [3] yields a neutron density $n_n = (3.3 \pm 0.3) \cdot 10^8$ cm^{-3}. This is the most stringent limitation for n_n which has been obtained so far.

[1] R.R. Winters, F. Käppeler, K. Wisshak, A. Mengoni, G. Reffo, Astrophysical Journal **300** (1986) 41

[2] K. Wisshak, F. Voß, F. Käppeler, G. Reffo, Report KfK 4899 (1991), Kernforschungszentrum Karlsruhe; Phys. Rev. C (in press)

[3] F. Käppeler, R. Gallino, M. Busso, G. Picchio, C.M. Raiteri, Astrophysical Journal **354** (1990) 630

4. ORIGIN OF $^{180}Ta^{m}$ AND THE TEMPERATURE OF THE s-PROCESS

ZS. NEMETH*, F. KÄPPELER, G. REFFO**

Despite of numerous studies over the past decade, the origin of $^{180}Ta^{m}$, the rarest isotope in nature, has not been revealed yet. This isotope is so much less abundant than the typical yields of all processes contributing to this mass region, that it probably owes its existence to a delicate interplay between the nuclear physics and the physical condition during its production. It is this sensitivity, which makes the origin of $^{180}Ta^{m}$ an important probe for a variety of nucleosynthesis sites.

The proposed mechanisms for producing $^{180}Ta^{m}$ are summarized in fig.1. The two light arrows from the right indicate the claims for an origin $^{180}Ta^{m}$ by the p- and ν-processes. While $^{180}Ta^{m}$ is generally not obtained in p-process calculations using parametrized scenarios, a more recent study [1] of a realistic model for the type II supernova SN1987A indicates for the first time a significant p-process yield of $^{180}Ta^{m}$. On the other hand, calculations of neutrino-induced nucleosynthesis in SN II explosions do also show $^{180}Ta^{m}$ production [2].

At present, reliable predictions can only be made for a possible neutron capture origin of $^{180}Ta^{m}$ (indicated by heavy arrows in fig.1), due to the availability of relevant experimental information. There are three ways of producing $^{180}Ta^{m}$ by neutron capture processes :

(i) A small fraction of the r-process beta decay chain at A = 180 feeding the 8^{-} isomer in ^{180}Hf could, in principle, result in sufficient $^{180}Ta^{m}$ production. However, there is ample experimental evidence that the corresponding branching in the decay of ^{180}Lu is compatible with zero, thus excluding an r-process origin of $^{180}Ta^{m}$.

(ii) Following the s-process path through the hafnium isotopes, Beer and Ward [3] suggested to produce $^{180}Ta^{m}$ by feeding the 8^{-} isomer in ^{180}Hf via s-process neutron captures in ^{179}Hf. Also this route was shown to be not efficient enough, yielding at most 22% of the observed $^{180}Ta^{m}$ abundance.

(iii) An important alternative was proposed by Yokoi and Takahashi [4], who found that ^{179}Hf becomes unstable under s-process conditions against beta decay from excited states. This results in a finite $^{179}Ta/^{179}Hf$ ratio, that is determined by the temperature (via the beta decay rate of ^{179}Hf) and the electron density in the stellar plasma (via the electron capture rate of ^{179}Ta). Neutron captures on ^{179}Ta lead then partly to $^{180}Ta^{m}$ and partly to the short-lived ground state of ^{180}Ta.

Through the second path, this scenario provides also an s-process contribution to ^{180}W, that was previously considered as a pure p-process isotope. Normalizing the s-process flow to the observed abundances of ^{180}W and $^{180}Ta^{m}$ could, therefore, constrain neutron density, temperature, and electron density in the s-process.

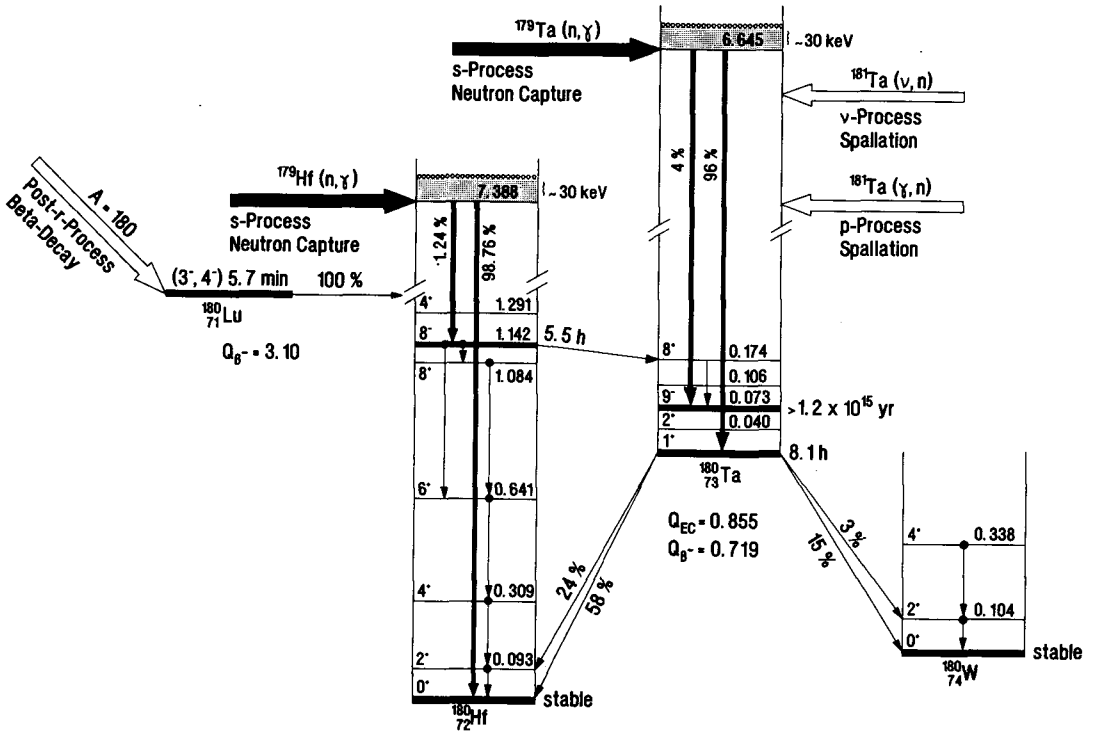

Fig.1: Level structure of the relevant A=180 isobars and the possible production processes of $^{180}Ta^{m}$ (energies are given in MeV). The r-process does not contribute the to the abundance of $^{180}Ta^{m}$ since $^{180}Hf^{m}$ is not populated in the β-decay of ^{180}Lu.

In the present work, two crucial aspects of the solution proposed by Yokoi and Takahashi [4] are investigated. First, the question is addressed whether $^{180}Ta^{m}$ can survive under s-process conditions or whether it might be quickly destroyed by equilibration with the short-lived ground state. It was found by photoexcitation measurements, that thermal equilibration between the short-lived ground state and the almost stable isomer is **not** achieved for temperatures lower than $5 \cdot 10^{8}$ K. This means, that $^{180}Ta^{m}$ is practically stable under all plausible s-process conditions of relevance for the mass region beyond A=90.

Secondly, the stellar neutron capture rates are calculated with a refined statistical model approach in order to quantify the s-process flow to $^{180}Ta^{m}$ and ^{180}W. These calculations include the total (n,γ) cross sections of ^{179}Ta and $^{180}Ta^{m}$.

These results allowed for a considerably refined description of the s-process flow in the mass region $178<A<184$, which is characterized by the important

branching at A = 179. The classical approach has been shown to yield ambiguous solutions for the production of $^{180}Ta^{m}$, even if the additional constraint is met, that not more than about 30% of the ^{180}W abundance should be produced in the s-process. It was found that there is a rather sharp temperature limit at $3 \cdot 10^{8}$ K : For *lower* temperatures, the branching at A = 179 remains unimportant, resulting in a marginal production of $^{180}Ta^{m}$. This solution is compatible with the predictions of current stellar models for low mass stars of low metallicity. At temperatures slightly *higher* than $3 \cdot 10^{8}$ K, $^{180}Ta^{m}$ can efficiently be produced in the s-process. Such temperatures, which are expected for stars of higher metallicity, are obtained from the s-process branchings, which can be interpreted as thermometers.

A distinction between the two possible interpretations of the origin of $^{180}Ta^{m}$ and the related consequences would require either reliable and quantitative p- and/or v-process calculations (which can hardly be expected in the near future), or a further improvement of the temperature estimates via the classical model. Given the recent progress in experimental techniques, the second possibility may be more promising. For the case of the branching at A = 179 further efforts have to concentrate on the experimental determination of the neutron capture rates of ^{179}Ta and $^{180}Ta^{m}$, on a critical assessment of the stellar beta decay rates, in particular the of ^{179}Hf, and on a measurement of the branching ratio in the decay of the 8^{-}isomer in ^{180}Hf. With these improvements, the origin of $^{180}Ta^{m}$ will be an important clue to the identification of the s-process site, and will allow to establish constraints for the p-and v-processes, as well.

[1] N. Prantzos, M. Hashimoto, M. Rayet, M. Arnould, Astron. Astrophys. **238** (1990) 455

[2] S.E. Woosley, D.H. Hartmann, R.D. Hoffman, W.C. Haxton, Astrophysical Journal **356** (1990) 272

[3] H. Beer, R.A. Ward, Nature **291** (1981) 308

[4] K. Yokoi, K. Takahashi, Nature **305** (1983) 198

* Institute of Isotopes, Budapest, Hungary

** ENEA, Laboratorio Dati Nucleari, Bologna, Italy

5. MEASUREMENT OF THE ^{180}W (n, γ) ^{181}W CROSS SECTION

H. BEER, F. KÄPPELER

The origin of ^{180}W is traditionally ascribed to p-process nucleosynthesis. However, according to Yokoi and Takahashi [1], a significant s-process contribution is also possible by a branching at ^{179}Hf via the sequence

$$^{179}Hf(\beta^-)\,^{179}Ta\,(n,\gamma)\,^{180}Ta^g(\beta^-)\,^{180}W$$

provided the s-process conditions (temperature, neutron- and electron density) allow for the β decay of the terrestrially stable isotope ^{179}Hf [2].

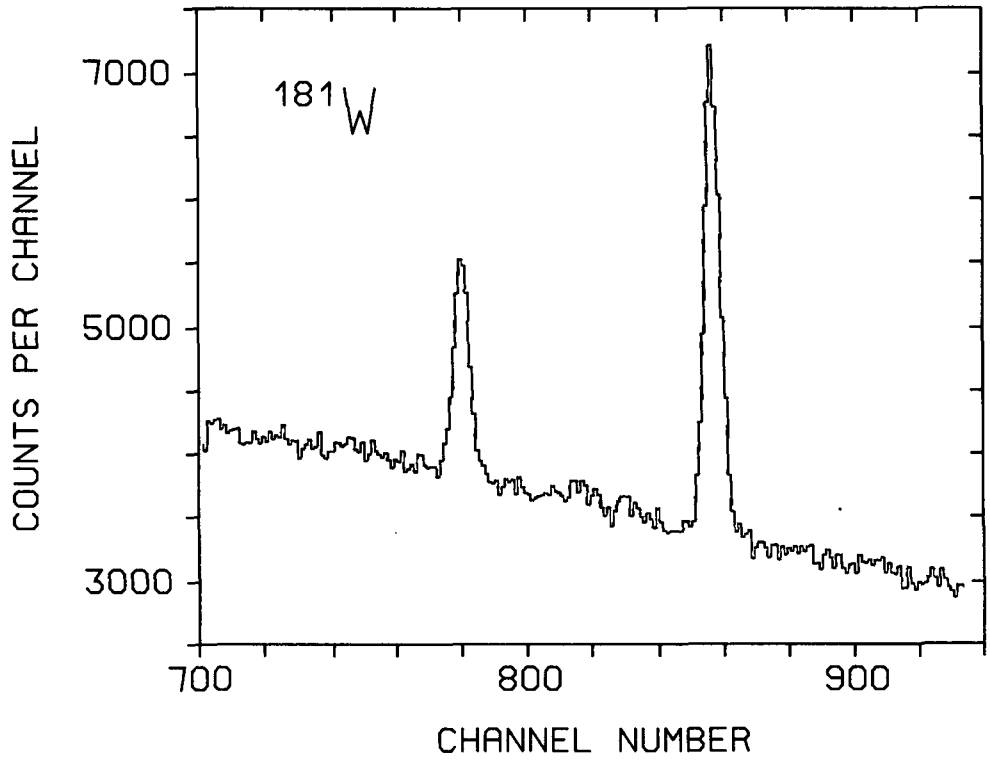

Fig.1 : The γ ray lines of the ^{181}W decay at 136.17keV and 152.21 keV, respectively, counted after the activation.

For a quantitative determination of the s-process part of the ^{180}W abundance, the ^{180}W destruction rate is needed. This quantity was measured by the activation technique at the Karlsruhe 3.75 MV Van de Graaff accelerator. For this purpose a 100 mg ^{180}W sample (enrichment 13.5%) was irradiated over a period of 7 days.

The produced ^{181}W activity was counted with a HPGe detector via a γ-ray line at 152.21 keV [intensity per decay = (0.084 + 0.003) %].

The cross section was determined relative to the ^{197}Au standard. The sample was sandwiched between two thin Au foils which were exchanged after three days of irradiation by fresh foils to avoid saturation of the Au activity. In fig.1, two characteristic γ-ray lines from the ^{181}W decay are shown.

In order to check the measurements for systematic uncertainties, three additional activations on ^{186}W were performed with tungsten of natural isotopic composition using the same conditions for neutron irradiation. Two of these measurements were carried out with thin metallic foils, and in the third measurement 100 mg of natural W powder was used simulating exactly the ^{180}W measurement.

For ^{180}W we derived a Maxwellian averaged capture cross section $\sigma = 624 \pm 29$ mb at 25 keV. This result is within quoted uncertainties in agreement with the respective value $\sigma = 603 \pm 27$ mb, calculated from the time-of-flight data of Bokhovko et al. [3] for kT = 25keV.

[1] K. Yokoi, K. Takahashi, 1987, Nature, **305** (1987), 198

[2] Zs. Németh, F. Käppeler, Astrophysical Journal (in press)

[3] M.V. Bokhovko, L.E Kazakov, V.N. Kononov, Problems of Atomic Sci. and Technology, Series on Nuclear Constants, Moscow (1986), No. 1, p. 39

KERNFORSCHUNGSZENTRUM KARLSRUHE
INSTITUT FÜR MATERIALFORSCHUNG

1. Fusion Materials Research and Related Nuclear Data Needs

S. Cierjacks, K. Anderko, K. Ehrlich

In continuation of the previous work, the significance of nuclear data for basic materials research with regard to radiation resistivity and low-activation properties was evaluated in more detail [1,2]. In general, important nuclear data needs arise from the necessity to quantify radiation damage effects [3] by a few "standard" irradiation parameters such as (1) displacement damages in terms of displacements per atom (dpa), (2) helium and hydrogen gas production rates in terms of atom parts per million (He-appm), (3) solid foreign element production rates, also in atom parts per million and (4) "effective" flux and fluence levels. Two other general tasks which are related to further nuclear data needs are neutron dosimetry in complex irradiation environments and the renewed investigations of high-intensity, high-energy candidate neutron sources for end-of-life fusion materials testing.

The second major objective of current materials research programs, the optimization of suitable radiation-resistant structural materials as so-called low-activation (LA) versions, is another important source for extensive data needs [4]. Concerning neutron data, two main groups of data are required: (a) data needed for the determination of space- and component-dependent neutron fluxes and (b) data required for the estimate of radioactivities and their related radiological quantities such as surface γ-dose rate, decay heat and biological hazard, induced in fusion reactors and simulation irradiation environments. For materials activation in fusion reactors not only all kinematically possible neutron-induced reactions, but also so-called sequential (x,n) reactions must be considered as demonstrated in previous work from our group [5]. The treatment of such reactions required large additional nuclear data libraries (see Section 3) not previously contained in any of the existing activation files.

Due to the lack of appropriate neutron sources for fusion materials testing, current irradiation experiments are largely based on simulation irradiation methods: In addition, to fission neutrons from thermal and fast fission reactors and spallation neutrons from operating spallation sources, light- and heavy-ion beams from existing medium-energy accelerator facilities are also widely used. In all these cases a major task is the transfer of simulation radiation results to fusion reactor conditions. Neutron irradiation methods with extended spectra require additional neutron data for the energy range 20 MeV to ~1 GeV. The energy of light- and heavy-ion beams is in many cases below ~ 50 MeV, but in more recent studies also energies in excess of 100 MeV are utilized. For this kind of irradiations a large variety of nuclear reaction and decay data is also required for interactions of up to 100-MeV light- and heavy-ions with the components of fusion materials.

2. The Influence of Sequential (x,n) Reactions on Integral Element Activities Produced in Fusion Reactors

S. Kelzenberg, S. Cierjacks, P. Obložinský [1], S. Ravndal

The previous investigations on the influence of the so-called "sequential (x,n) reactions" [4] (SxRs) have been extended. In the past, the contributions of such reactions had been neglected in all calculations.

Two years ago, our group had, for the first time, demonstrated for a few special examples that SxRs can significantly contribute to the integral radioactive inventory produced in a fusion reactor material [5]. This observation required more systematic investigations of the importance and the range of validity of SxRs in terms of reaction types and mass range of target materials. Due to the progress in the production of the necessary new data libraries for the purpose the systematic studies of the (p,n), (d,n) and (α,n) sequential reactions on all stable and radioactive nuclides with $T_{1/2} \geq 1$ day for the mass range $9 \leq A \leq 100$ could be finalized by the end of 1991. These investigations showed that SxRs are important for about 30 % of the elements from B to Mo [4] where these reactions dominate all or some of the integral radiological quantities in major portions of the cooling time from 10^{-3} to 10^{6} years. Unfortunately, the previous systematics indicated also that SxRs could not be restricted to the main three reactions (p,n), (d,n) and (α,n) on the light and medium weight nuclei only. This required a further extension of the new KfK libraries with respect to target masses and reaction types. After completion of the extended data libraries, further investigations on the influence of SxRs were performed in the reporting period. Extension to the reactions (t,n), (^{3}He,n), (d,2n) and (t,2n) on target nuclides with $9 \leq A \leq 100$ and $T_{1/2} \geq 1$ day, and study of all possible sequential reactions (p,n), (d,n), (α,n), (t,n), (^{3}He,n), (d,2n) and (t,2n) on nuclides with $100 \leq A \leq 209$, gave another large number of important SxRs (24 reactions for the mass range $100 \leq A \leq 209$) which cannot be neglected in future activation calculations of fusion materials. With the new work the systematic investigations of SxRs is now largely complete, except for the following special cases: (1) Although effective "pseudo" cross sections are available from complete reaction data, about 100 SxRs cannot yet be treated in FISPACT calculations due to the lack of decay data for residual nuclides, (2) For (t,n) and (^{3}He,n) reactions present spectrum data need to be improved according to other reaction mechanism in the first and second step of SxRs, such as pick-up and break-up. (3) The treatment of special reactions in the light nuclides below $A \leq 12$. A special example of this kind is ^{7}Li (t,γ) or the two member chain ^{7}Li (t,n); ^{9}Be (n,γ) leading both to ^{10}Be with $T_{1/2} = 1.6 \times 10^{6}$ yr. The involved cross sections are difficult to measure, and their theoretical estimates are also not trivial.

3. Extension of the New KfK Data Libraries for the Complete Treatment of Sequential (x,n) Reactions in Fusion Activation Calculations

P. Obložinský [1], S. Cierjacks, S. Kelzenberg, B. Rzehorz

A complete study of the influence of SxRs on element activation in fusion reactor relevant neutron spectra required large new data libraries for the following three types of nuclear and atomic data: (1) Neutron-induced charged-particle emission cross sections as a function of both the incident neutron and the outgoing charged-particle energy. (2) Energy-dependent charged-particle neutron-emission cross sections. (3) Differential charged particle ranges for all light ions produced in neutron reactions with fusion relevant spectra. For realization of such libraries the data of type (1) were split into two contributions (factorization): (a) neutron-induced excitation functions and (b) normalized charged-particle emission spectra, thus resulting in two independent libraries. Excitation functions for the one-step (n,x) reactions are taken from the European Activation File (EAF) maintained by the Petten laboratory. (This choice allows to use always the latest, most updated EAF version; presently EAF-2). For the required normalized charged particle spectra, a new library KFKSPEC, fully based on nuclear model calculations with the ALICE code was created. The same approach is adopted to produce the starter library KFKXN for all required charged-particle reaction cross sections. A complete set of differential

charged-particle ranges is generated by using the Ziegler formalism, and the improved KfK code PRAL, to produce the library KFKSTOP. The present status of the three new KfK libraries, after all extensions finalized before March 1992 [4,6-10], is summarized in Table I. For each library the table contains information on the range of elements, the number of isotopes, the energies and types of particles covered, the number of spectra, reactions and total data points, as well as the achieved status of completion.

TABLE I: Summary of the current status for the three KfK data libraries KFKSPEC, KFKXN and KFKSTOP.

KFKSPEC Library: Normalized (n,x) spectra

Quantity	Content
Elements	$Z \leq 84$
No. of isotopes	633 including 55 isomers (same as in EAF-1)
Incident neutron energies E_n	18.5, 17.1, 16.1, 14.7, 14.0, 13.2, 12.4, 11.3, 10.2, 9.3, 8.4, 7.6, 6.9, 5.9, 5.1, 4.3, 3.3, 2.4, 1.5, 0.6 MeV
Outgoing charged particles	x = p, d, t, ^{3}He, α
Charged particle energies E_x	0.5, 1.5, ... , 23.5 MeV
No. of spectra	63 300
No. of data points	more than 1.5 million
Status	version KFKSPEC-2

KFKXN Library: (x,n) production cross sections

Quantity	Content
Elements	$Z \leq 84$
No. of isotopes	633 including 55 isomers (same as in EAF-1)
Reactions (x,n) for	x = p, d, t, ^{3}He, α
Reactions (x,2n) for	x = d, t (c. s. are large compared to (d,n) and (t,n))
Charged particle energies E_x	0.5, 1.5, ... , 23.5 MeV
No. of reactions	4 431
No. of data points	about 106.000
Status	version KFKXN-2

KFKSTOP Library: Differential ranges of charged particles

Quantity	Content
No. of elements	92
Charged particles	x = p, d, t, ^{3}He, α
Charged particle energies E_x	0.5, 1.5, ... , 23.5 MeV ΔR_x steps given in cm for 1 MeV enegy loss
No. of data points	11 040
Status	KFKSTOP final version

4. Code Development for a Global Treatment of Neutron-Induced (n,x) and Sequential (x,n) Reactions with the European Reference Code FISPACT

S. Ravndal, S. Kelzenberg, P. Obložinský [1], S. Cierjacks

In order to handle sequential (x,n) reactions in standard activation calculation with the European Reference Code FISPACT, a new algorithm was developed at KfK [6,11]. This algorithm makes use of the introduction of so-called "pseudo" cross sections describing a two-step reaction process by a single cross-section equivalent number. Thus the new algorithm avoids any change in the intrinsic structure of the original FISPACT inventory code. Application of this particular treatment transfers the successive two-step reaction calculations into an extensive code package producing the largely extended input information prior to the start of the main program for inventory calculations. A flow chart of the new program structure used for the simultaneous treatment of one- and two-step activation reactions is shown in Fig. 1. The essential program extensions are concentrated in the KfK processing code PCROSS [12,13] which combines the extended input information from the previously only treated (n,x) reactions and the transponed information for SxRs. All of the extended information is taken from the input files, the input parameter blocks and the supplementary KfK data libraries KFKSPEC, KFKXN and KFKSTOP. Using the new KfK processing code PCROSS, allows a complete coverage of all energetically possible (n,x) and sequential (x,n) reactions in the calculation of element activations. In addition, the KfK code can be used to prepare a common input data file of collapsed "effective" neutron and "pseudo" cross sections for kinematically complete inventory calculations of complex metallic alloys or other materials with any given composition of elements.

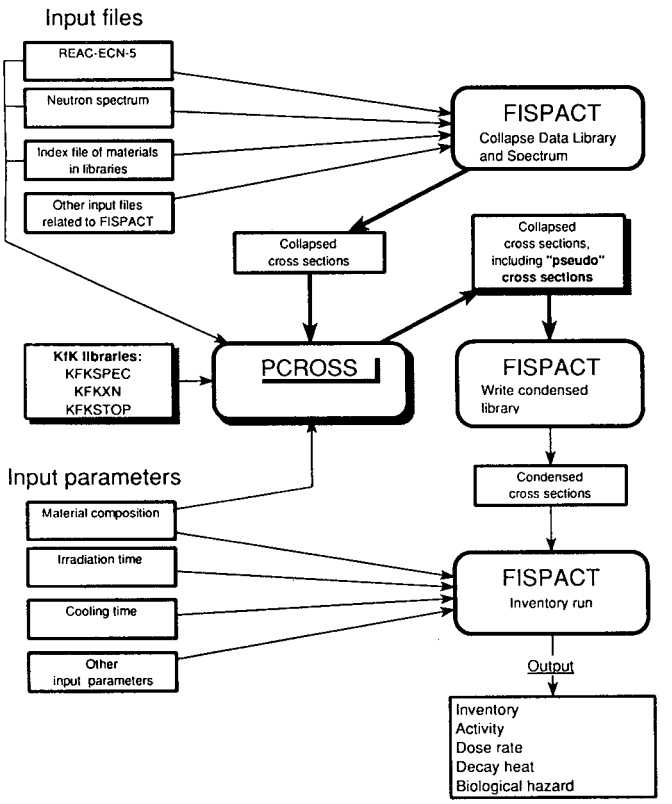

Fig. 1. Flow chart of the new program structure used for generalized calculations of one- and two-step activation reactions. The normal pathway of FISPACT calculations (neglecting SxRs) is marked on the right side. For details see text.

5. Integral Data Testing of Critical Activation Cross Sections

S. Kelzenberg, S. Cierjacks, P. Obložinský [1], J. Möllenbeck [2] G. Peters [2]

For integral data testing a new fast neutron facility had been set up at the Karlsruhe Isochronous Cyclotron (KIZ) by the end of 1990. Its use for data testing of critical activation cross sections needed for the development of LA Fe-, V-, and Cr-basis alloys has been continued during the last year. In general, this facility employs a 50-MeV cw deuteron beam bombarding a thick metallic target for production of strongly forward-peaked stripping neutrons. While in the first measurements a thick (fully absorbing) Cu-target was used for neutron production, this target was recently replaced by a 12-mm thick Be-target, which gives a significantly increased neutron yield. Utilization of a 30 - 50 μA cw deuteron beam provides total neutron intensities of 2.2 - 3.7 x 10^{14} n/s, respectively. The average energy of the resulting white neutron spectrum is close to 15 MeV. A typical neutron spectrum produced by bombardment of a thick Cu-target with a 50 MeV deuteron beam is shown in Fig. 2. The major portion of the "effective" neutron spectrum at the position of the activation target is dominated by the deuteron break-up (p-stripping reaction) in the energy range from ~ 3 - 35 MeV. Additional contributions arise from neutron evaporation ($E_n \lesssim 3$ MeV) and precompound emission ($E_n \gtrsim 35$ MeV).

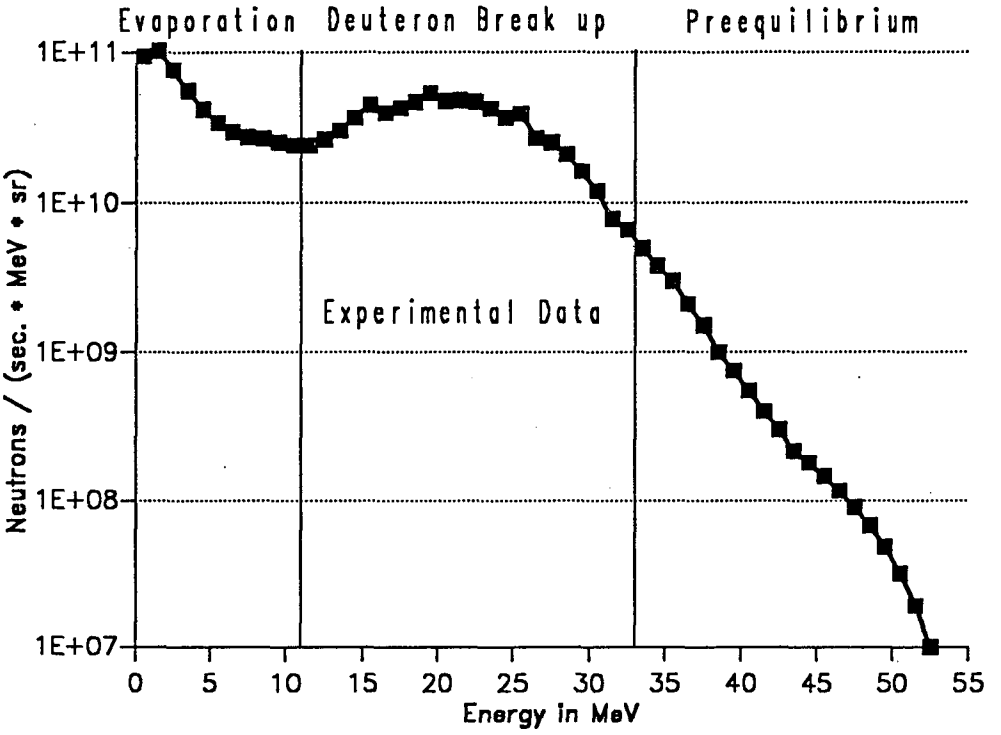

Fig. 2. Neutron spectrum produced by bombardment of a thick Cu target with a 50-MeV cw deuteron beam. The given result is the "effective" neutron spectrum in the position of the 1x1 cm^2 activation sample. For spectrum contributions see text.

Integral experiments have been performed for the verification of the important sequential reaction

$$^{19}F(n, \alpha y) \rightarrow {}^{19}F(\alpha,n)^{22}Na$$

and for the validation of the most important activation reactions on natural V. Data analysis of the experimental results for the sequential (α,n) reaction on F has been finalized [14]. The measured ^{22}Na-activity gave good agreement with the calculated one, using the known "effective" neutron spec-

trum and the new KfK nuclear data libraries. The evaluation of the measured V element activities is in progress.

In the reporting period, two other improvements of the test facility have been initiated: (1) For replacement of the rather old Ge(Li) detector device, a new high-purity Ge detector with improved specifications has been ordered. (2) In addition, a new calibrated Si(Li) detector device was bought. This provides for the future an important additional possibility for data testing of induced radioactivities from nuclides decaying by electron capture only.

6. Study of High-Intensity, High-Energy Neutron Sources for End-of-Life Fusion Materials Testing

S. Cierjacks, E. Daum, Y. Hino [3)], K. Ehrlich, S. Kelzenberg

In continuation of our previous investigations on the KfK proposal for a novel t-H_2O source [15-18], comparative neutron calculations for this and an equivalent d-Li source have been finalized. Extensive calculations of uncollided differential space-dependent flux spectra were carried out for two reference designs selected by the members of IEA Working Group on Neutron Sources. In the first reference case a one beam, one target source configuration was chosen; the common target beam power was 3.5 MW for both types of sources, provided by a rectangular beam of 3 x 1 cm² dimension with uniform intensity. The second reference case was a two-beam, two-target source configuration, a total target beam power of 17.5 MW (8.75 MW on each target) and a uniform intensity, 3 x 7 cm² beam shape. A typical result from our latest calculations for the two-source reference case is shown in Fig. 3 which displays

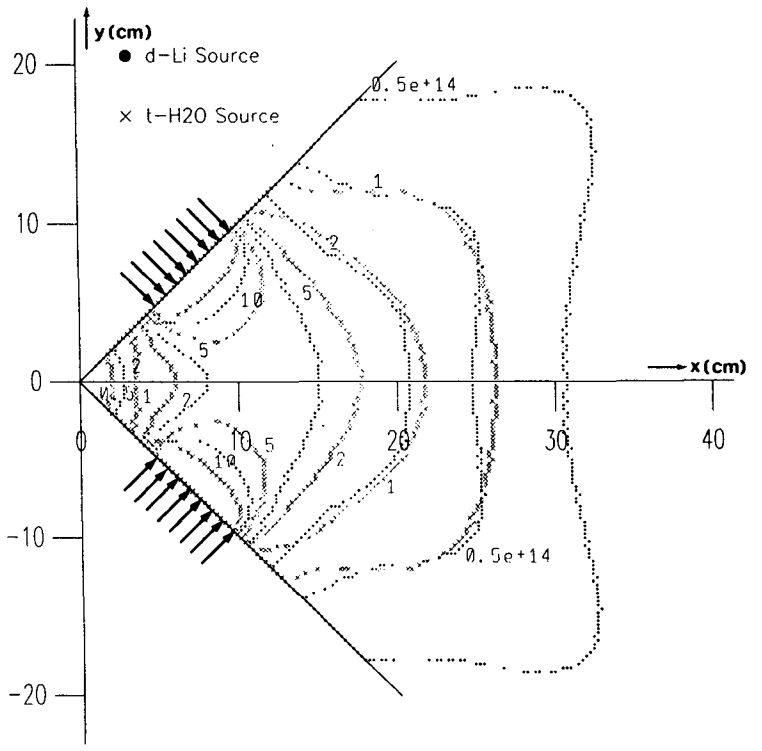

Fig. 3. Comparison of flux contours calculated for equivalent reference designs of d-Li and t-H_2O sources, respectively. For the reference design a two-beam two-target configuration with 8.75 MW beam power each was chosen. Uncollided minimum neutron fluxes are mainly less than a factor of 2 smaller for the t-H_2O than for the d-Li source.

the contours for 5 given "minimum-flux" levels. It can be seen that the minimum fluxes at the same test cell positions are typically less than a factor of 2 smaller for the t-H_2O than for the d-Li source. The higher flux levels for the d-Li source are, however, only achieved on the expense of a correspondingly high fraction of neutrons with energies in the range $14 \leq E_n \leq 50$ MeV which are highly undesirable for fusion materials testing. A comparison of flux-dependent volumes for the d-Li and the t-H_2O source are given in Table II.

TABLE II: Flux-dependent volumes for five characteristic minimum flux levels of comparable d-Li and t-H_2O sources (reference design as in Fig. 3).

Flux Level Φ_{min} ($cm^{-2}\,s^{-1}$)	Volume (cm^3)	
	d-Li	t-H_2O
1×10^{15}	104	51
5×10^{14}	550	185
2×10^{14}	2.430	1.035
1×10^{14}	6.220	2.580
5×10^{13}	12.200	6.190

The volumes for the minimum energy-integrated fluxes are also by about a factor of two different and this ratio varies slightly with flux levels. Volumes with the flux levels $\geq 10^{15}$, which are of interest for accelerated irradiations, differ by a factor of 2.05 for t-H_2O and d-Li sources, respectively.

7. Nuclear Data for Accelerator-Driven Transmutation Technology

S. Cierjacks

Accelerator-based transmutation of high-level radioactive waste from light-water reactors has become an interesting alternative concept to nuclear incineration in thermal and fast fission reactors. Present concepts and objectives of accelerator-driven transmutation technology cover a wide range of ideas ranging from the utilization of proton-induced spallation and/or fission reactions to high-intensity thermal and fast neutron fields produced by medium-energy proton, light-ion or electron beams, or by muon-catalyzed fusion. For studying such concepts in more detail, a large number of new or more precise nuclear data is needed. The general needs and the most urgent requirements for crucial system-driving properties have been critically examined in a survey paper [19] prepared for the OECD/NEA Specialist's Meeting on Accelerator Based Transmutation, held at PSI, Switzerland, in March 1992. An important category of required nuclear data are spallation and fission cross sections for medium-energy protons on heavy-mass target nuclei and of critical nuclei contained in the high-level waste (actinides and fission products). Additional data needs exist for more precise double differential neutron-production cross sections as well as n- and γ-transport cross sections. The needs are most urgent for the range 20 MeV to $\sim$ 1.5 GeV. A special problem in transmuter concepts based on extremely high thermal neutron fluxes ($> 10^{16}\,cm^{-2}\,s^{-1}$) is radiation damage in the primary spallation-target container. More reliable damage calculations require additional displacement and gas production (H, He) cross sections for radionuclide production that are important for determining the overall mass balance of a transmutation system (i.e. the ratio of waste material transmuted to radioactive material cre-

ated). Finally, there is an immediate need for low energy neutron reaction cross section of ^{137}Cs, ^{238}Np (and possibly other short-lived actinides) for which significant and system-driving uncertainties still exist.

---

[1] On leave from the Institute of Physics, SAS, 842 28 Bratislava, Czechoslovakia

[2] Kernforschungszentrum Karlsruhe, Hauptabteilung Zyklotron

[3] Present address: Electrotechnical Laboratory, 1-1-4 Umezono, Ibaraki, Japan

References

[1] S. Cierjacks; Nuclear data needs for low-activation fusion materials development; Fus. Engrg. Design 13, 229 (1990).

[2] S. Cierjacks, K. Ehrlich; Invited paper on "Nuclear data for fusion materials research"; in Proc. Int. Conf. on Nuclear Data for Science and Technology, Jülich, FRG, May 13-17, 1991, Ed. S.M. Qaim, Springer-Verlag Berlin Heidelberg, p. 259, 1992.

[3] A. Möslang, S. Cierjacks, R.Lindau; Invited paper on "Test of fusion reactor materials with cyclotrons and presentation of the Karlsruhe Dual-Beam Facility", in Proc. of the 12th Intern. Conf. on Cyclotrons and their Applications, Berlin, FRG, May 8-12, 1989, Eds. B. Martin, K. Ziegler, World Scientific Publishing Co., p. 545, 1991.

[4] S. Cierjacks, P. Obložinský, B. Rzehorz, Nuclear data libraries for the treatment of sequential (x,n) reactions in activation calculations; Proc. IEA Workshop on Low Activation Materials, Culham, UK, April 7-12, 1991, Session 3, Contribution c), 12 pages, (1991).

[5] S. Cierjacks, Y. Hino; The importance of sequential (x,n) reactions on element activation of fusion reactor materials; J. Nucl. Mater. 170, 134 (1990).

[6] S. Cierjacks, P. Obložinský, S. Kelzenberg, B. Rzehorz; Development of a novel algorithm and production of new nuclear data libraries for the treatment of sequential (x,n) reactions in fusion materials activation calculations; submitted to Fusion Technology.

[7] S. Cierjacks, P. Obložinský, B. Rzehorz; Nuclear data libraries for the treatment of sequential (x,n) reactions in fusion materials activation calculations; Kernforschungszentrum Karlsruhe Report, KfK-4867, Juli 1991.

[8] P. Obložinský, S. Cierjacks, S. Kelzenberg, B. Rzehorz; Production of new nuclear data libraries for low-activation materials development from statistical/preequilibrium model calculations, OECD/NEA Topical Conf. on Nuclear Data for Fusion Reactor Technology, Karlsruhe, FRG, October 23, 1991; Proc. to be published.

[9] P. Obložinský, M.B. Chadwick, Invited poster on "Calculations of photoproduction reactions"; in Proc. Int. Conf. on Nuclear Data for Science and Technology, Jülich, FRG, May 13-17, 1991, Ed. S.M. Qaim, Springer-Verlag Berlin Heidelberg, p. 842, 1992.

[10] P. Obložinský; Reply to comment on "preequilibrium emission of hard photons in proton-nucleus reactions"; Phys. Rev. C44, 923 (1991).

[11] P. Obložinský, S. Cierjacks, S. Ravndal, S. Kelzenberg; A novel algorithm for the treatment of sequential (x,n) reactions in standard activation calculations. OECD/NEA Topical Conf. on Nuclear Data for Fusion Reactor Technology, Karlsruhe, FRG, October 23, 1991; Proc. to be published.

[12] S. Ravndal, P. Obložinský, S. Kelzenberg, S. Cierjacks User manual for the KfK Code PCROSS; Kernforschungszentrum Karlsruhe Report, KfK-4873, August 1991.

[13] S. Ravndal, P. Obložinský, S. Kelzenberg, S. Cierjacks Reference manual for the KfK Code PCROSS; Kernforschungszentrum Karlsruhe Report, KfK-4956, December 1991.

[14] S. Kelzenberg, S. Cierjacks, P. Obložinský, J. Kaneko; Integral data testing of critical activation cross sections for fusion materials development at the Karlsruhe Isochronous Cyclotron. OECD/NEA Topical Conf. on Nuclear Data for Fusion Reactor Technology, Karlsruhe, FRG, October 23, 1991; Proc. to be published.

[15] S. Cierjacks, Y.Hino, M. Drosg; Proposal for a high-intensity 14-MeV cutoff neutron source based on the $^{1}H(t,n)^{3}He$ reaction; Nucl. Sci. Eng. 106, 183 (1990).

[16] S. Cierjacks, Y. Hino; Additional studies related to the proposal for a novel high-intensity 14-MeV cutoff neutron source based on the $^{1}H(t,n)^{3}He$source reaction; Proc. Internat. Panel on 14-MeV Intense Neutron Sources Based on Accelerators for Fusion Materials Study; Eds. A. Miyahara, F.W. Wiffen; Tokyo, Japan, January 14-16, 1991, Nagoya National Institute for Fusion Science Report, NIFS-WS-2, p. 147, 1991.

[17] S. Cierjacks, Y. Hino; Differential flux and spectrum calculations for a novel high-intensity 14-MeV cutoff neutron source based on the $^{1}H(t,n)^{3}He$ source reaction; Acta Physica Hungarica 69 (3-4), 285 (1991).

[18] F.H. Coensgen, G.P. Lawrence, S. Cierjacks; Invited poster on "Neutron sources for fusion materials testing"; in Proc. Int. Conf. on Nuclear Data for Science and Technology, Jülich, FRG, May 13-17, 1991, Ed. S.M. Qaim, Springer-Verlag Berlin Heidelberg, p. 395, 1992.

[19] S. Cierjacks; Invited paper on "Cross section measurements, integral validation experiments and nuclear model code developments of importance to accelerator-based transmutation"; OECD/NEA Specialists' Meeting on Accelerator-Based Transmutation, Paul-Scherrer Institute (PSI), Würenlingen/Villigen, Switzerland, March 24-26 1992, Proc. to be published.

[20] S. Cierjacks, Ed., Proc. of an OECD/NEA Topical Conf. on Nuclear Data for Fusion Reactor Technology, Karlsruhe, FRG, October 23, 1991; in press.

[21] D.L. Smith (Ed.); A. Michaudon, S. Cierjacks, A.B. Smith (General Eds.); "Probabilities, statistics and data uncertainties in nuclear science and technology"; OECD/NEA Nuclear Data Committee Series on Neutron Physics and Nuclear Data in Science and Technology, Volume 4, American Nuclear Society, Inc., Kensington, USA, 1991.

KERNFORSCHUNGSZENTRUM KARLSRUHE
INSTITUT FÜR NEUTRONENPHYSIK UND REAKTORTECHNIK

Nuclear Data Evaluation

1. Evaluation of Neutron Cross Sections for ^{238}U in the Unresolved Resonance Region: JEF-2 Data Tests

F.H. Fröhner

The differential data tests of the recent ^{238}U neutron cross section evaluation in the unresolved resonance range (10 - 200 keV) [1] have been supplemented by comparisons of the observed temperature dependence of thick-sample transmission and self-indication data with JEF-2 based Monte Carlo calculations. The table shows, as an example, the agreement obtained for transmissions measured with cooled and heated samples relative to room temperature transmissions [2]. A report on our JEF-2 tests against differential data has been issued [3]. The state of the capture cross section of ^{238}U as judged by a NEANDC/NEACRP task force was presented at the Jülich conference [4]. All recent major evaluations of the resonance-averaged neutron capture cross section (JEF-2, ENDF/B-VI, JENDL-3 and the latest version of BROND) agree to within 1 - 1.5 % in the unresolved resonance region.

Table 1. Thick-sample transmission ratios and uncertainties of Byoun et al. (1972) (transmission of cooled or heated sample relative to room temperature transmission, thermal expansion included) compared with Monte Carlo results based on JEF-2. Statistical uncertainties of Monte Carlo results are roughly 0.7 % .

Energy Range (keV)	Temperature Ratio (K : K)	Sample Thickness (at./b) 0.03155 (6.6 mm)	0.06206 (13.1 mm)	Temperature Ratio (K : K)	Sample Thickness (at./b) 0.03155 (6.6 mm)	0.06206 (13.1 mm)
15.2-16.8	77:293	1.005±0.012 1.007	1.010±0.011 1.018	973:293	1.026±0.018 1.018	1.010±0.011 0.992
22.6-25.0		1.007±0.012 1.005	0.999±0.012 1.019		1.029±0.012 1.022	1.011±0.012 0.998
33.8-37.3		0.999±0.013 1.003	1.008±0.013 1.010		1.026±0.013 1.023	1.016±0.013 1.005
50.4-55.7		0.997±0.013 1.002	1.004±0.012 1.011		1.029±0.012 1.024	1.023±0.013 1.007
83.1-91.9		0.998±0.015 1.001	0.992±0.014 1.003		1.023±0.014 1.023	1.021±0.015 1.023

2. Assignment of Uncertainties to Resonance Parameters for Structural Materials

F.H. Fröhner

The JEF-2/EFF-2 resonance parameter files for ^{54,56,57,58}Fe that were recently updated [5]are being supplemented with uncertainty files. These are needed e.g. for an assessment of the adequacy of the steel shielding planned for the New European Torus (NET). As far as possible the uncertainties are taken from the resonance analyses on which the evaluations are based. Especially at higher energies, however, many gaps in the resonance parameter tables had to be filled with model-generated values. In particular most radiation widths for the various partial waves were unknown and had to be based on sample averages determined at low energies. In those cases uncertainties were derived from the sample distributions observed at low energies. The uncertainty assignments are complete for ^{56}Fe and ^{54}Fe, and preliminary ENDF-formatted covariance files have been constructed. Work on the other isotopes is in progress.

[1] F.H. Fröhner, Nucl. Sci. Eng. **103** (1989) 119

[2] T.Y. Byoun, R.C. Block, T. Semler, Proc. Meet. New Developments in Reactor Physics and Shielding Calculations, Kiamesha Lake 1972, CONF-720901 (1972) Book 2, p. 1115

[3] F.H. Fröhner, KfK 4911 (1991); shorter version to be published in Nucl. Sci. Eng., Aug. 1992

[4] Y. Kanda, Y. Kikuchi, Y. Nakajima, M.G. Sowerby, M.C. Moxon, F.H. Fröhner, W.P. Poenitz and L.W. Weston, Proc. Int. Conf. Nucl. Data in Sci. and Technol., Jülich 1991 (in print)

[5] F.H. Fröhner, NEANDC(E)-312-U Vol. V (1990) p. 15

INSTITUT FÜR KERNPHYSIK,
ARBEITSGRUPPE STRAHLUNGSTRANSPORT
FORSCHUNGSZENTRUM JÜLICH

Validation of Several Intranuclear Cascade Models by Measurements of Neutrons, Protons and Pions Induced by Medium-Energy Proton Bombardment of Aluminum and Iron

P. Cloth, V. Drüke, D. Filges, D. Theis *

*ISKP, University of Bonn

This study aimed on the validation by comparison of HETC-Bertini /1/ /2/ and the NUCRIN/GHEISHA codes available in GEANT /3/ and MICRES /4/ on one side and double differential experimental cross sections for neutrons /5/, protons /6/ and pions /7/. We present a selection of data comparisons in Figs. 1 and 2. Fig. 1 shows comparisons of double differential proton and neutron production cross sections for incident protons at 558 MeV and 800 MeV energy on iron. Fig. 2 shows comparisons of double differential pion production cross sections (π^+,π^-) for incident protons at 730 MeV energy on aluminum.

There are considerably differences between model predictions, but it is clearly seen that the HETC-Bertini and MICRES models fit the data comparatively best. MICRES is an extended version of the HETC-Bertini model.

References

/1/ P. Cloth et al., KFA-Report Jül-2203 (1988)
/2/ T.W. Armstrong, K.C. Chandler, Nucl. Sci. Eng. 49, 110 (1972)
/3/ R. Brun et al., CERN DD/EE/84-1 (revised), (1987)
also H. Fesefeldt, RWTH Aachen PITHA 85/02 (1985)
R. Brun et al., Proc. of the LHC Workshop Vol. 1, ECFA 90-133, CERN 90-10 (1990)
/4/ D. Theis to be published
/5/ W. Amian et al., Proc. Int. Conf. on Nuclear Data for Science and Technology, Jülich, 13.-17. Mai 1991
/6/ S.M. Beck and CA. Powell, Langley Research Center, NASA-TN-D-8119, Washington DC, (1976)
/7/ D.A.F. Cochran et al., Phys. Rev. D, No. 11, Vol. 6 3085 (1972)

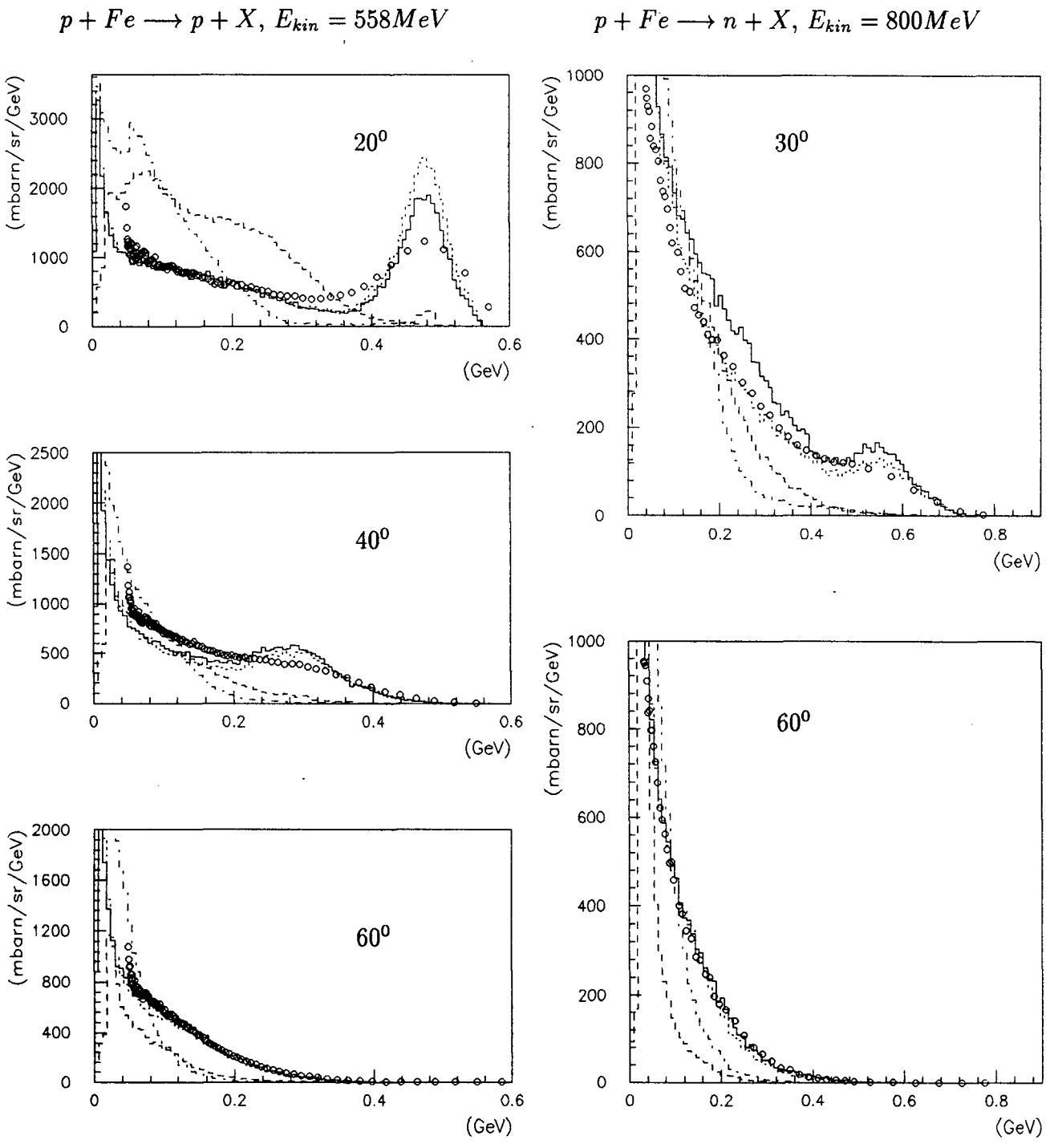

Figure 1: double differential proton and neutron production cross sections for incident proton on iron at 558 MeV and 800 MeV respectively. Proton data are from Beck et al., neutron data are from Amian et al. Full line Bertini code, dashed line NUCRIN, dotted line MICRES and dashed dotted line GHEISHA.

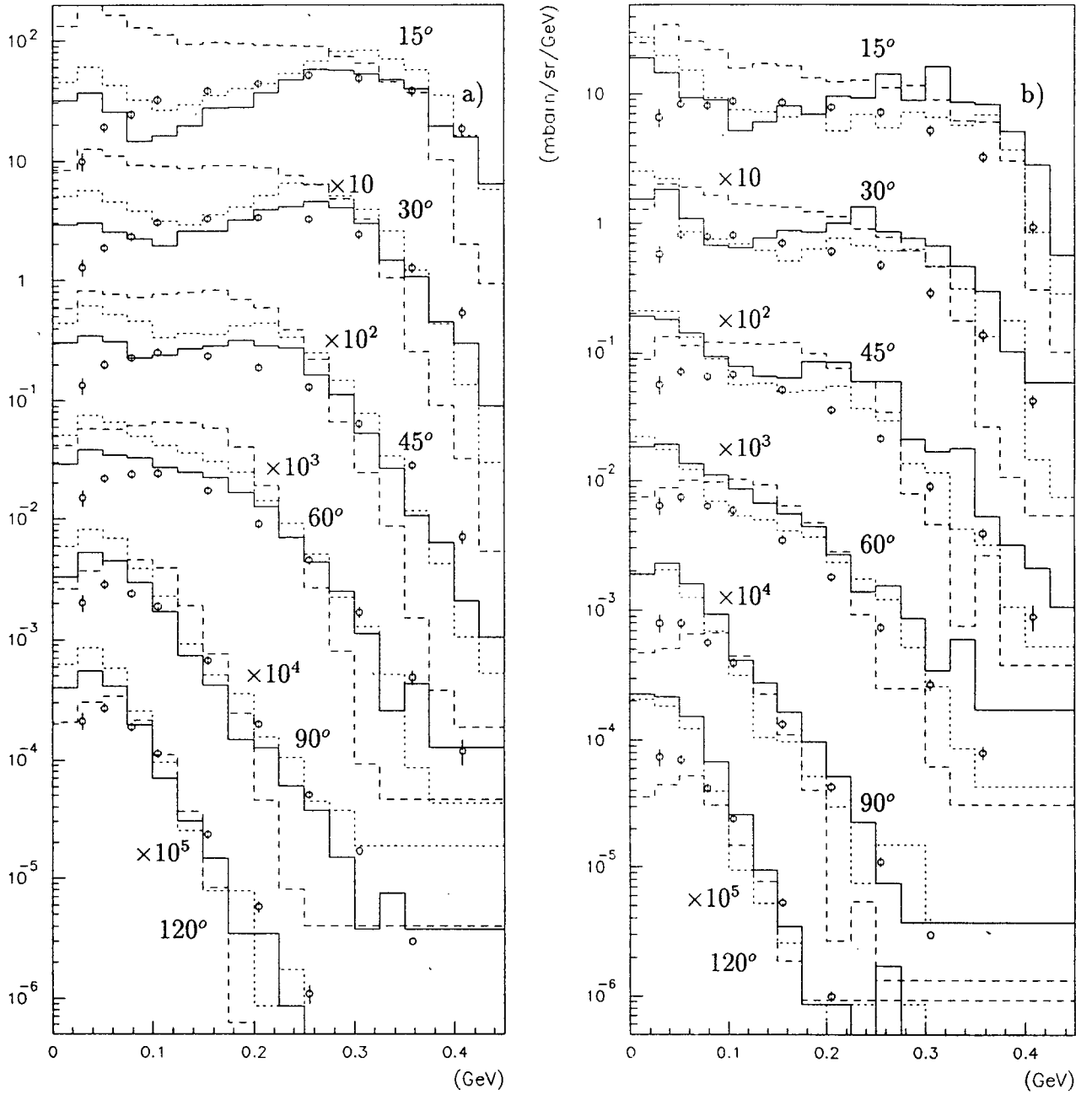

Figure 2: double differrential pion production cross sections for the bombardment of aluminium by 730 MeV protons, a) $p + Al \longrightarrow \pi^+ + X$, b) $p + Al \longrightarrow \pi^- + X$. Full line Bertini model, dashed line NUCRIN and dotted line MICRES. Data are from Cochran et al.

INSTITUT FÜR NUKLEARCHEMIE
FORSCHUNGSZENTRUM JÜLICH

1. Studies of Complex Particle Emission Reactions

B. Scholten, B. Neumaier, S.M. Qaim, G. Stöcklin

In continuation of our fundamental studies on nuclear reactions involving complex particle emission [cf. 1,2] the excitation function of the $^{209}Bi(p,^{7}Be)^{203}Hg$ reaction was investigated in the energy range below 45 MeV. The radiochemical methods for the separation of ^{7}Be were improved and measurements are now underway at energies below the threshold of the proton induced fission of ^{209}Bi ($\sim$ 20 MeV).

The $(n,^{7}Be)$ reaction was studied radiochemically with 53 MeV d(Be) neutrons on the target elements Al, Si, V, Fe, Co, As, Nb and Au. The systematic trends observed in complex particle emission reaction cross sections are shown in Fig. 1. It is evident that the higher the mass of the complex particle, the lower is its emission probability. Furthermore, whereas the

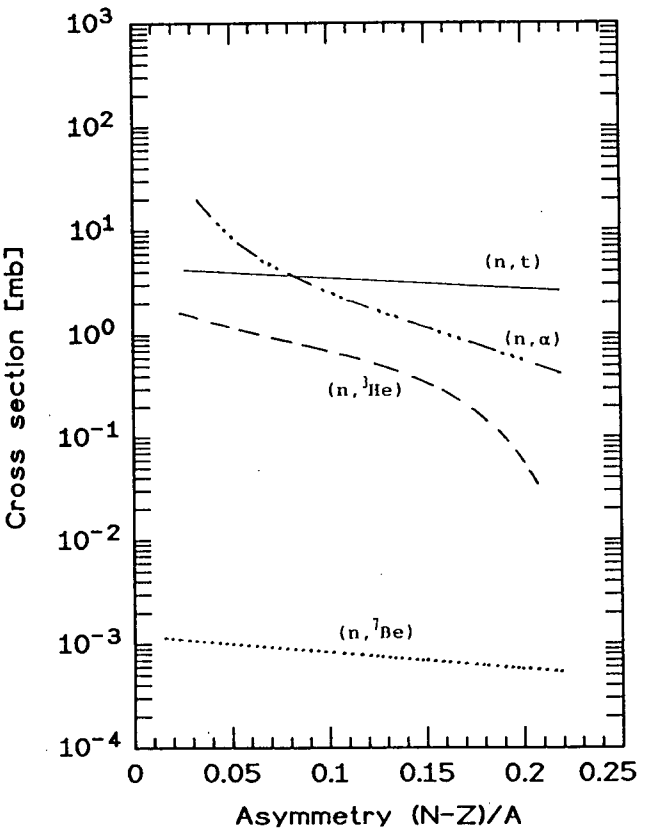

Fig. 1 Systematics of (n,t), $(n,^{3}He)$, (n,α) and $(n,^{7}Be)$ reaction cross sections induced by 53 MeV d(Be) breakup neutrons on medium and heavy mass nuclei.

cross sections for the first chance emission of individual α- and ^{3}He-particles are in the range of 0.1 to 1 mb, those for the emission of bound ^{7}Be-particles are by three orders of magnitudes smaller (0.5 - 1 μb). Further studies in this direction are in progress.

2. Isomeric Cross Section Ratios

I. Birn, S. Sudár, S.M. Qaim

Continuing our studies on isomeric cross section ratios we investigated the formation of the isomeric pair ^{75m,g}Ge in several neutron induced reactions, namely ^{75}As(n,p)^{75m,g}Ge, ^{76}Ge(n,2n)^{75m,g}Ge and ^{78}Se(n,α)^{75m,g}Ge. The neutron energy range covered was 5 to 12 MeV. Nuclear model calculations are underway at the Technical University Dresden.

The formation of the isomeric pair ^{58m,g}Co was investigated in several neutron and charged particle induced reactions like ^{58}Ni(n,p)^{58m,g}Co [cf. 3], ^{59}Co(n,2n)^{58m,g}Co, ^{58}Fe(p,n)^{58m,g}Co, ^{57}Fe(d,n)^{58m,g}Co and ^{55}Mn(α,n)^{58m,g}Co. The energy ranges covered were: n (5-12 MeV), p (5-20 MeV), d (4-14 MeV), α (8-28 MeV). Nuclear model calculations on the excitation functions and isomeric cross section ratios are in progress at the Kossuth University, Debrecen, Hungary.

3. Cross Section Data Relevant to Fusion Reactor Technology

I. Birn, M. Bostan, S.M. Qaim
(Relevant to request identification numbers: 742127R, 742129R, 761055R, 812002F, 861120F, 861175F, 861184F)

Excitation functions of the following neutron induced reactions were measured from threshold to 12 MeV: ^{45}Sc(n,p)^{45}Ca, ^{45}Sc(n,α)^{42}K, ^{45}Sc(n,2n)$^{44m+g}$Sc, ^{55}Mn(n,α)^{52}V, ^{75}As(n,α)^{72}Ga, ^{80}Se(n,α)$^{77m+g}$Ge. The aim was twofold: a) to test nuclear models, b) to obtain data of some relevance to fusion reactor technology. Further analysis of the data is in progress.

Measurements on the ^{151}Eu(n,2n)^{150m}Eu and ^{159}Tb(n,2n)^{158}Tb reactions in the energy range of 8 to 10.5 MeV were completed in cooperation with Kossuth University, Debrecen, Hungary, under an IAEA-research agreement [4].

A systematic analysis of the previously measured (n,p) cross sections on isotopes of titanium [cf. 5] showed that the calculational code EXIFON can reproduce all the excitation functions well [6].

Detailed radiochemical studies on the $^{63}Cu(n,p)^{63}Ni$ process are in progress. Thick copper samples irradiated with neutrons in the energy range of 7 to 10 MeV are processed chemically and the soft β^- emitter ^{63}Ni ($T_{1/2}$: 100 y; E_{β^-} = 70 keV) is separated. Its activity is measured by low-level β^- counting.

4. Excitation Functions Relevant to Radioisotope Production

F. Szelécsényi, F. Rösch, Z. Kovács, F. Tárkányi, S.M. Qaim, G. Stöcklin

In continuation of our studies [cf. 7-10] on the production of medically important short-lived radioisotopes we measured for the first time excitation functions for the formation of longer-lived β^+ emitting radioisotopes ^{64}Cu and ^{86}Y at a small-sized cyclotron.

Investigations on the $^{64}Ni(p,n)^{64}Cu$ ($T_{1/2}$ = 12.7 h) reaction were carried out using the stacked-foil technique. The electrolytic method developed to obtain thin films of ^{62}Ni on Au-backing (described in the last Progress Report) was used also in the case of highly enriched (95 %) ^{64}Ni. Results show that the optimum energy range for the production of ^{64}Cu is E_p = 12 → 9 MeV and a ^{64}Cu-yield of 6.7 mCi (248 MBq)/μAh can be expected.

The β^+ emitting radioisotope ^{86}Y ($T_{1/2}$ = 14.7 h) allows to measure the uptake kinetics and individual dosimetry, preparatory to therapeutic investigations with the β^- emitter ^{90}Y. The cross section data for the $^{86}Sr(p,n)^{86}Y$ reaction were measured using 96 % enriched ^{86}Sr. Thin $^{86}SrCO_3$ samples (used in the form of a stack) were prepared by a special sedimentation technique. The results of measurements are shown in Fig. 2. The optimum energy range for the production of ^{86}Y is E_p = 14 → 10 MeV; the thick target yield of ^{86}Y amounts to 10.8 mCi (400 MBq)/μAh and the level of $^{87,88}Y$ impurities to 3 %.

Cross section measurements on highly enriched gas targets were continued in cooperation with ATOMKI Debrecen, Hungary. Work is in progress on the excitation functions of $^{78}Kr(p,\alpha)^{75}Br$ and $^{78}Kr(p,x)^{77}Br$ processes.

5. General

The Institute acted as host to the International Conference on Nuclear Data for Science and Technology, Jülich, May 1991. A total of 328 persons from 37 countries and five international organizations participated. About 300 invited and contributed papers were presented. The Proceedings have been recently published [11].

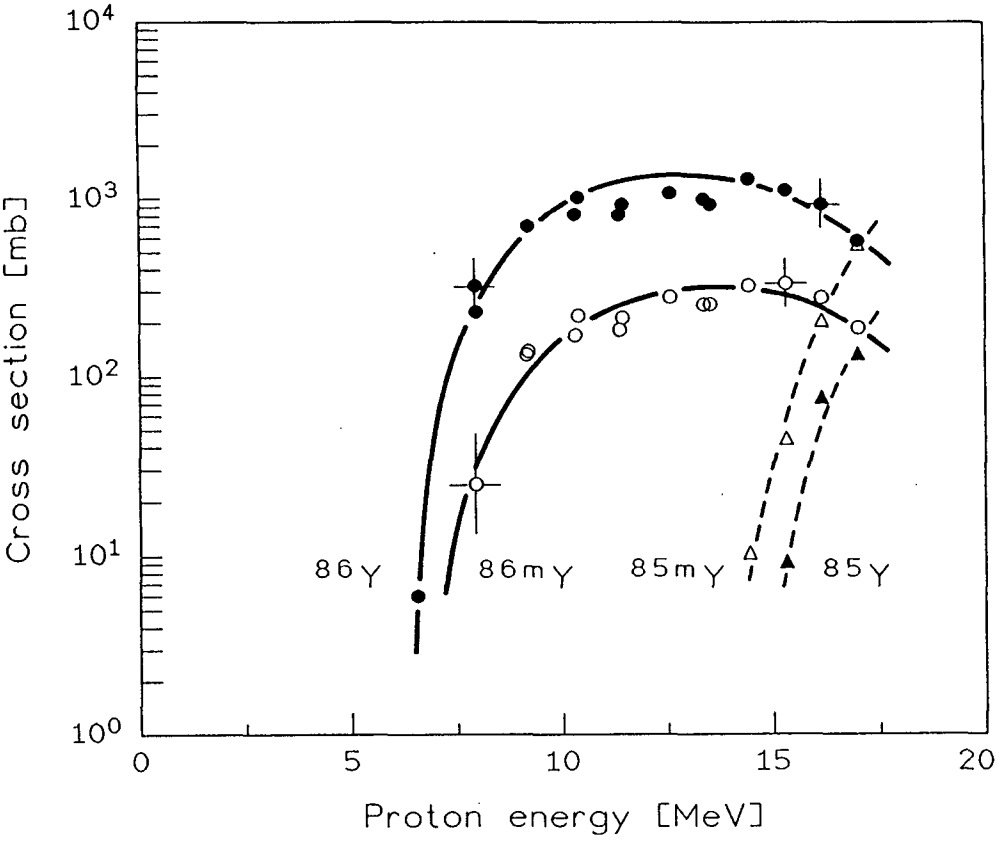

Fig. 2 Excitation functions for the formation of ^{86m}Y, ^{86}Y, ^{85m}Y and ^{85}Y in proton induced nuclear reactions on ^{86}Sr.

References

[1] S.M. Qaim, R. Wölfle: Excitation function of $^{139}La(n,^3He)^{137}Cs$ reaction near its threshold, Acta Physica Hungarica 69 (1991) 137

[2] B. Scholten, S.M. Qaim, G. Stöcklin: ^7Be emission in proton and neutron induced reactions, Proc. Int. Conf. on Nuclear Data for Science and Technology, Jülich, May 1991 (S.M. Qaim, Editor), Springer Verlag, Berlin/Heidelberg, 1992, p. 711

[3] S. Sudár, J. Csikai, S.M. Qaim, G. Stöcklin: Neutron activation cross sections for $^{60}Ni(n,p)^{60m}Co$, $^{60}Ni(n,p)^{60m+g}Co$ and $^{58}Ni(n,p)^{58m}Co$ reactions in the 5 to 12 MeV energy range, Proc. Int. Conf. on Nuclear Data for Science and Technology, Jülich, May 1991 (S.M. Qaim, Editor), Springer Verlag, Berlin/Heidelberg, 1992, p. 291

[4] S.M. Qaim, F. Cserpák, J. Csikai: Cross sections of $^{151}Eu(n,2n)^{150m}Eu$ and $^{159}Tb(n,2n)^{158}Tb$ reactions near their thresholds, Appl. Radiat. Isotopes, in press

[5] S.M. Qaim, N.I. Molla, R. Wölfle, G. Stöcklin: Differential and integral cross section measurements of some (n, charged particle) reactions on titanium, Proc. Int. Conf. on Nuclear Data for Science and Technology, Jülich, May 1991 (S.M. Qaim, Editor), Springer Verlag, Berlin/Heidelberg, 1992, p. 297

[6] N.I. Molla, S.M. Qaim, H. Kalka: Excitation functions of $^{46-50}$Ti(n,p)$^{46-50}$Sc processes, Phys. Rev. C, in press

[7] Z. Kovács, F. Tárkányi, S.M. Qaim, G. Stöcklin: Production of 6.5 h ^{82m}Rb via the ^{82}Kr(p,n)-process at a low-energy cyclotron - A potential substitute for ^{82}Rb, Appl. Radiat. Isotopes 42 (1991) 831

[8] Z. Kovács, F. Tárkányi, S.M. Qaim, G. Stöcklin: Cross sections of proton induced nuclear reactions on Kr gas relevant to the production of medically important radioisotopes ^{81}Rb and ^{82m}Rb, Proc. Int. Conf. on Nuclear Data for Science and Technology, Jülich, May 1991 (S.M. Qaim, Editor), Springer Verlag, Berlin/Heidelberg, 1992, p. 601

[9] F. Tárkányi, Z. Kovács, S.M. Qaim, G. Stöcklin: Production of ^{38}K via the ^{38}Ar(p,n)-process at a small cyclotron, Appl. Radiat. Isotopes 43 (1992) 503

[10] H. Piel, S.M. Qaim, G. Stöcklin: Excitation functions of (p,xn)-reactions on ^{nat}Ni and highly enriched ^{62}Ni: Possibility of production of medically important radioisotope ^{62}Cu at a small cyclotron, Radiochimica Acta, in press

[11] S.M. Qaim (Editor), Proc. Int. Conf. on Nuclear Data for Science and Technology, Jülich, May 1991, Springer Verlag, Berlin/Heidelberg, 1992

INSTITUT FÜR SICHERHEITSFORSCHUNG
FORSCHUNGUNGSZENTRUM ROSSENDORF

1. Neutron Data Check by Sample Reactivity Measurements in Reactor Configurations with Specially Designed Neutronic Properties

K.Dietze[1], G.Hüttel[2], E.Lehmann[3]

Within the framework of our data testing program [1,2,3], final sample reactivity measurements with fission product nuclides, structural materials and standards were performed in the central experimental channel of the fast substitution lattices SEG-7A and SEG-7B inserted in the Rossendorf fast-thermal coupled facility RRR/SEG. Both SEG-7 configurations are characterized by an extremly soft neutron spectrum, an approximately energy-independent adjoint (neutron importance) spectrum and k_∞ near 1. The calculated neutronic spectra are shown in Fig.1.
In regard of the soft neutron spectra, these configurations are well suited for a neutron data check in the resonance region. Because of the nearly energy-independent adjoint spectra, the scattering contribution to the sample reactivity is very small. Therefore the investigations are mainly focussed on as well the validation of capture cross-sections and capture self-shielding factors as on the solution of the U-235/B-10 discrepancy reported in the literature [4] and also found in all our previous configurations [5].
In detail, the method of analysis is described in [5,6,7]. Preliminary results of C/E-ratios obtained with fission product nuclides are given in Table 1. Further analysis with latest neutron data is restrictedly going on.

Table 1. Preliminary ratios of the calculated to experimental central reactivity worths (CRW) for FP nuclides in the SEG-7A, related to the C/E-ratio of boron-10. The uncertainties of the experimental values E are between 8 - 15%.

FP nuclide	C/E-ratios of CRW					
	SOKRATOR-88	JENDL-1	JENDL-2	ENDF/B-IV	ENDF/B-V	ENDL-78
Mo-95	0.78		0.78		0.74	
Mo-97	0.87	0.87			0.81	
Mo-98	0.97				1.01	
Rh-103	1.18			1.23		
Ag-109	0.95	1.00			0.92	0.96
Sm-149	1.58			1.09		

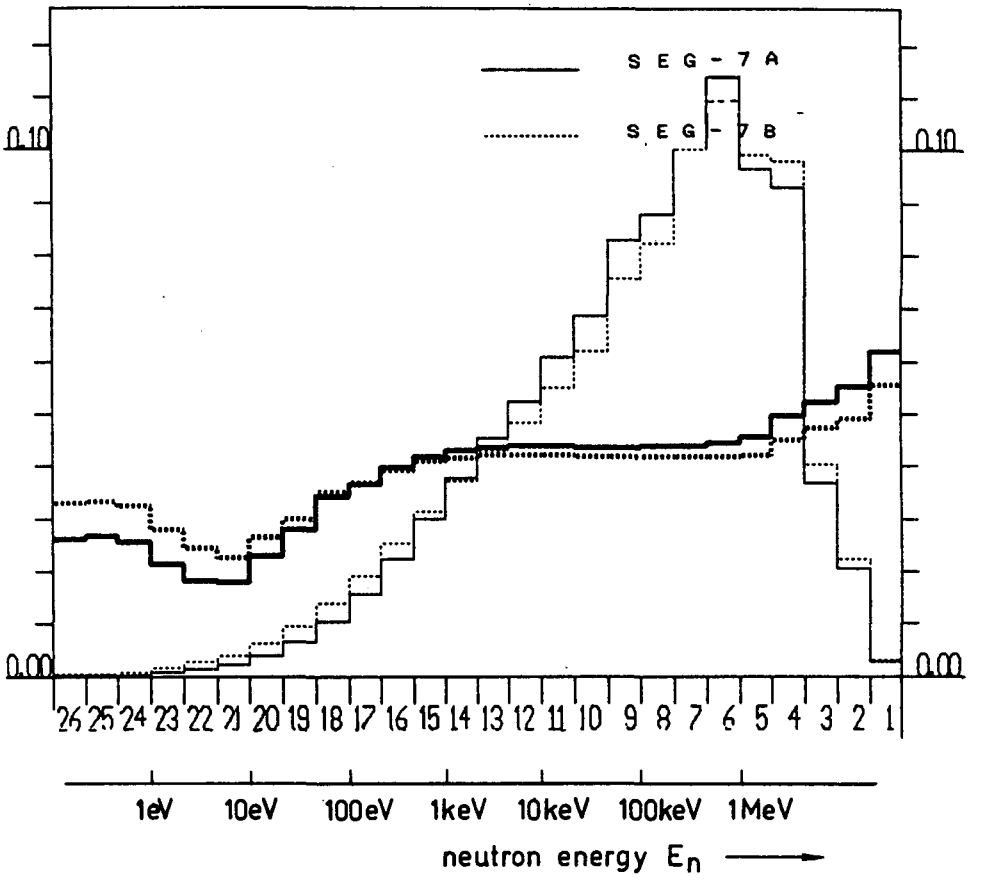

Fig.1. Neutron spectra and adjoint spectra of the SEG-7A and SEG-7B configurations in ABBN-group representation.

---

1) Forschungszentrum Rossendorf e.V., Institut für Sicherheitsforschung
2) Verein für Kernverfahrenstechnik und Analytik e.V., Rossendorf
3) Paul Scherrer Institut, CH-5232 Villigen PSI

References

[1] K.Dietze,W.Hansen,G.Hüttel,H.Kumpf,E.Lehmann,and D.Richter; Proc. of the Int. Conf. on Nucl. Data for Sci. and Techn., May 1991, Jülich/Germany.
[2] K.Dietze,G.Hüttel,H.Kumpf,and E.Lehmann; Progress Report on Nuclear Data Research in the F.R.Germany, NEANDC(E)-322, p.39, 1991.
[3] K.Dietze; Invited paper, OECD/NEA Specialists Meeting on Fission Product Nuclear Data, 25-27 May, 1992, JAERI/Japan, FZR Preprint 92-02, Rossendorf, May 1992.
[4] L.P.Abagyan,N.O.Bazazyanc,M.N.Nikolaev,A.M.Cibulya; Gruppovye Konstanty ..., Moskva, Energoizdat, 1981, p.123.
[5] K.Dietze,H.Kumpf; Kernenergie 34 (1991) p.1 (in German).
[6] K.Dietze,K.Fährmann,G.Hüttel,and E.Lehmann; Kernenergie 29 (1986) p.11.
[7] K.Dietze,K.Fährmann,W.Hansen,G.Hüttel,H.Kumpf,and E.Lehmann; Kerntechnik 53/2 (1988) p.143.

INSTITUT FÜR KERN- UND ATOMPHYSIK
TECHNISCHE UNIVERSITÄT DRESDEN

1. Evaluation and Analysis of 14.1 MeV Neutron Induced Double Differential Neutron Emission Cross Sections of ^{238}U [1)]

T. Elfruth, K. Seidel, S. Unholzer

Double-differential neutron emission cross sections (DDX) are of major importance for the design of D-T fusion reactor components. In particular, for fusion-fission hybrid reactor projects the 14 MeV neutron induced emission cross sections of ^{238}U are of interest. Moreover, the 14 MeV data are reference point for the evaluation of DDX at lower incidence energies. The data are needed with accuracies of $\lesssim$ 10 % [1].

With the procedure described in Ref. [2] the DDX were measured at E_o = 14.1 MeV incidence energy. Together with all other available experimental results [3-6] corrected to E_o = 14.1 MeV, if necessary, group-averaged evaluated DDX were derived in form of

$$\sigma(E,\vartheta) = \frac{\sigma(E)}{4\pi}\sum_{l=0}^{2}(2\cdot l+1)\cdot f_l\cdot P_l(cos(\vartheta))$$

The numerical values of $\sigma(E), f_1$ and f_2 and their uncertainties are presented in the Final Report of the CRP as report of the IAEA.
Evaluated data are compared in Fig. 1 with the experimental data used, in Fig. 2 with library data and in Fig. 3 with a theoretical analysis.

For the analysis σ(E) is calculated as sum of cross sections σ_i(E) of all possible neutron emission chances n_i. As shown in Fig. 4 at each stage of the deexciting system, neutron emission competes with γ-emission, and also with fission additionally leading to fission neutrons (n_f). The n_1 are assumed to be emitted in the pre-equilibrium and in the equlibrium phase of the reaction. Pre-equilibrium neutrons arise from multistep-direct (SMD) and from multistep-compound (SMC) processes. Their statistical treatment with the code EXIFON [7] includes as one- and two-step direct processes both, single-particle and collective excitations (2^+ and 3^- phonons). The SMC-neutron emission is calculated by solving the master equation from 5-exciton states up to the equilibrium of excited particles and holes. The n_2 and n_3 are emitted from the equilibrated system. The n_f are evaporated from the accelerated fragments. Not specific input parameters, but a surface-delta interaction of V_o = 19.4 MeV, r_o = 1.4 fm, the single-particle level density g = A/13 MeV^{-1} and phonon data from mass-number dependent systematics are used. The angular distribution is calculated with the assumption that the SMD-component is anisotropic and can be parametrized with the Kalbach-Mann-formula.

The neutron emission spectra were also calculated with the same parameters for $E_o = 6 \cdots 9.6$ MeV and are compared in Fig. 4 with experimental data. Additionally, the emission of neutrons from U in coincidence with fission events was calculated for $E_o = 6 \cdots 14.2$ MeV and is compared with experimental results in Fig. 4.

It can be seen that the model used describes the main emission components adequately. Starting from the DDX The evaluated DDX for $E_o = 14.1$ MeV, where the multitude of experimental results exists, satisfy the accuracy requirements. Codes like EXIFON can be used to improve the library data in the whole fast neutron emission region.

[1)] Part of the IAEA Co-ordinated Research Programme (CRP) on "Measurement and Analysis of 14 MeV Neutron-Induced Double-Differential Neutron Emission Cross Sections needed for Fission and Fusion Reactor Technology"

References

[1] Nuclear Data for Fusion Reactor Technology, in Proc. Adv. Group Meeting of the IAEA, Gaussig 1986, IAEA-TECDOC-487, IAEA, Vienna, 1988

[2] H. Al Obiesi et al., INDC(GDR)-058/L, IAEA, Vienna, 1990
T. Hehl, Thesis, TU Dresden, 1990

[3] J.L. Kammerdiener, Thesis, UCRL-51232, Livermore, 1972

[4] J. Voignier et al., CEA-3503 (1968) and EXFOR 21094.004 (1980)

[5] S. Guanren, in Proc. Adv. Group Meeting on Nuclear Theory for Application, Bejing, 1987

[6] D. J. Degtjarev et al., Jadernaja Fizika **34**(1981)299

[7] H. Kalka, INDC(GDR)-059/L, IAEA, Vienna, 1990

[8] V. Kornilov et al., in Proc. Conf. on Neutron Physics, 1980, Kiev, Vol. 3, p. 104, Moskva, 1980

[9] Zhou Zuying, private communication, 1992

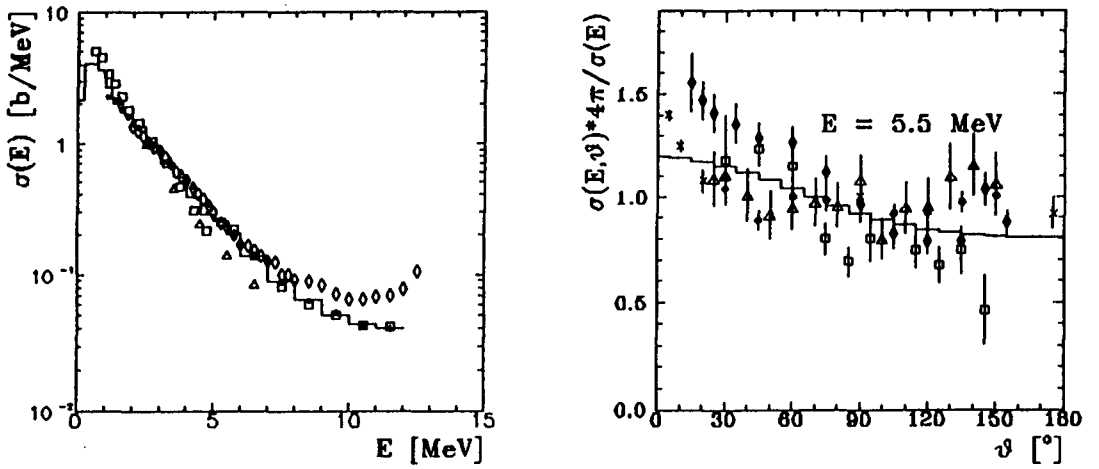

Fig. 1: Energy distribution σ(E) of the neutrons emitted after 14.1 MeV neutron bombardment and relative angular distribution at E = 5.5 MeV neutron emission energy.
Experimental data: □ [3], △ [4], ◇ [5], ∗ [6], (•) present work; evaluated experimental data: histogram ;

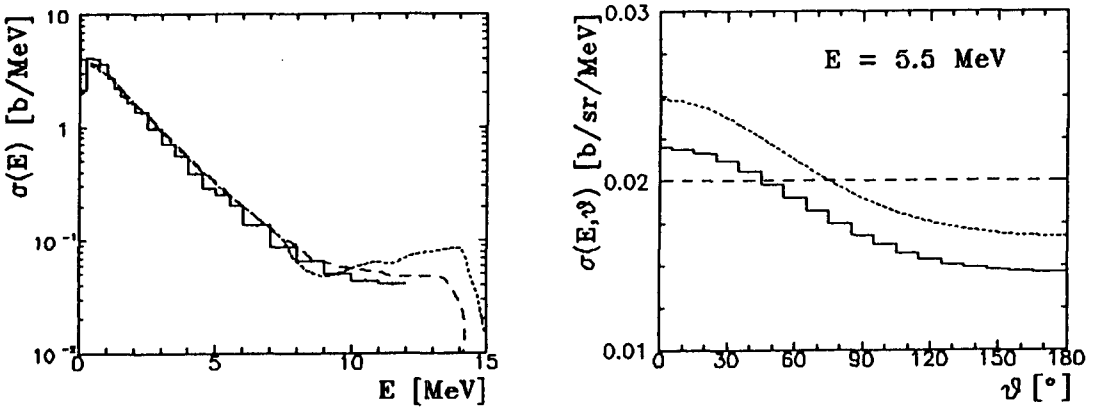

Fig. 2: Comparison of σ(E) and of the DDX at E = 5.5 MeV as evaluated from the experimental data at E_o = 14.1 MeV neutron incidence energy (histogram) with the data of the libraries ENDF/B-VI (short-dashed line) and ENDL-83 (dashed line).

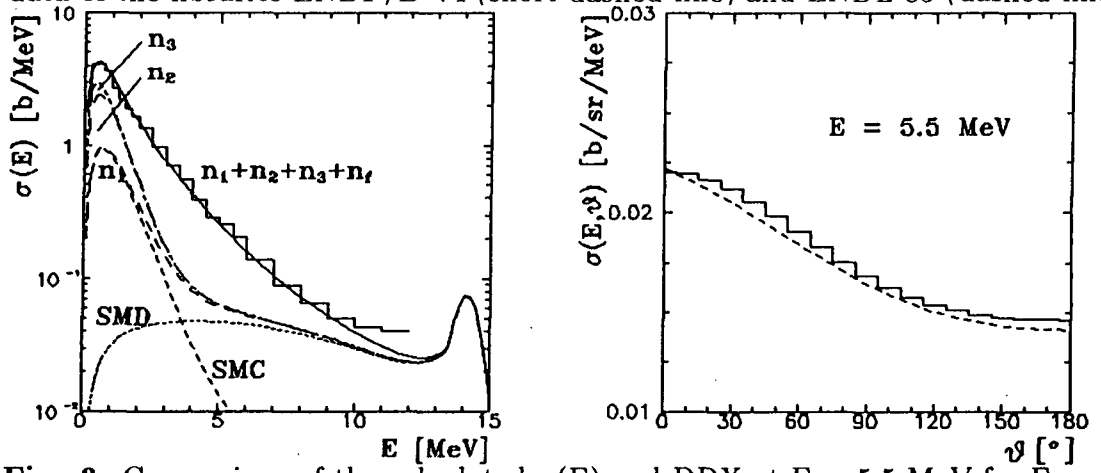

Fig. 3: Comparison of the calculated σ(E) and DDX at E = 5.5 MeV for E_o = 14.1 MeV neutron incidence energy with the evaluated experimental data (histogram).

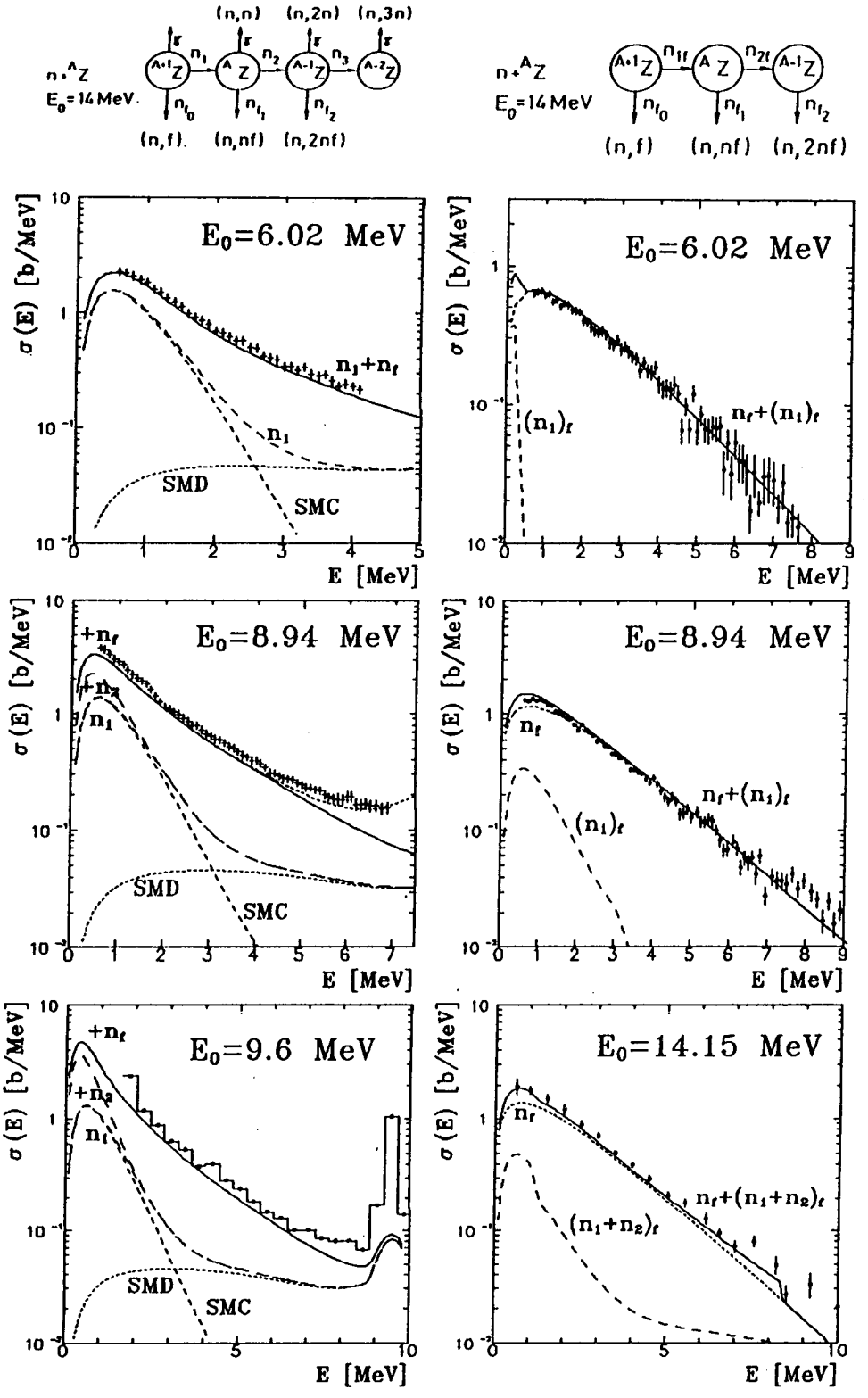

Fig. 4: Calculated σ(E) compared with experimental data for E_o = 6 ... 14 MeV. Left hand: total emission (exp. data of Ref. [8] (+) and Ref. [9] (•),respectively). Right hand: emission in coincidence with fission (exp. data of Ref. [8]). Designation of the neutron emission chances (at E_o = 14 MeV) in the upper part.

2. Evaluation of 14.1 MeV Neutron Induced Double-Differential Neutron Emission Cross Sections of ^{51}V [1)]

T. Elfruth, K. Seidel, S. Unholzer

Vanadium is one of the structure materials in fusion reactor designs. For neutron transport calculations of the reactor components energy- and angle-differential neutron emission cross sections (DDX) are needed with an accuracy of $\lesssim$ 10 % [1]. Comparing the recent experimental results at E_o = 14 MeV with the evaluated data of libraries (Fig. 1) significant differences of the spectral shapes and of the angular distributions are obvious. They exceed the data accuracy needed.

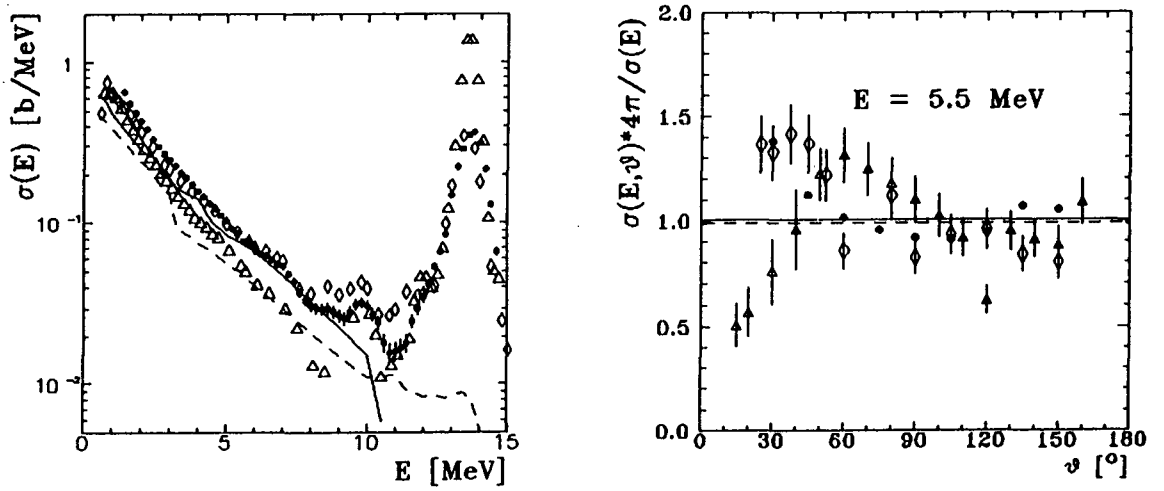

Fig. 1: Energy distribution of the neutrons emitted after 14 MeV neutron bombardment (left hand) and angular distribution at 5.5 MeV neutron emission energy (right hand).
Experimental data: • [2], △ [3], ◇ [4]. Library data: ENDF/B-VI (solid line), ENDL-83 (dashed line)

These experimental data are used for the evaluation of

$$\sigma(E,\vartheta) = \frac{\sigma(E)}{4\pi}\sum_{l=0}^{l_{max}}(2\cdot l+1)\cdot f_l\cdot P_l(cos(\vartheta))$$

at E_o = 14.1 MeV.
The procedure is described in the Final Report of the CRP published as report of the IAEA. σ(E), f_1 and f_2 (with restriction to l_{max} = 2) and their uncertainties are numerically presented in this report too.

The f_1 and f_2 can be parametrized by

$$f_1(E) = 0.002418\cdot E^2 - 0.002542\cdot E + 0.0122 \text{ , and}$$

$$f_2(E) = 0.0008425\cdot E^2 + 0.0009666\cdot E + 0.00513 .$$

The σ(E) have the accuracy needed for fusion reactor design. They are compared in Fig. 2 with the data of the libraries ENDL-83 and ENDF/B-VI. A calculation of σ(E) with the code EXIFON [5] taking into account statistical multistep-direct (SMD) and statistical multistep-compound (SMC) processes with global parameters is in better agreement with the evaluated experimental σ(E) than the library data.

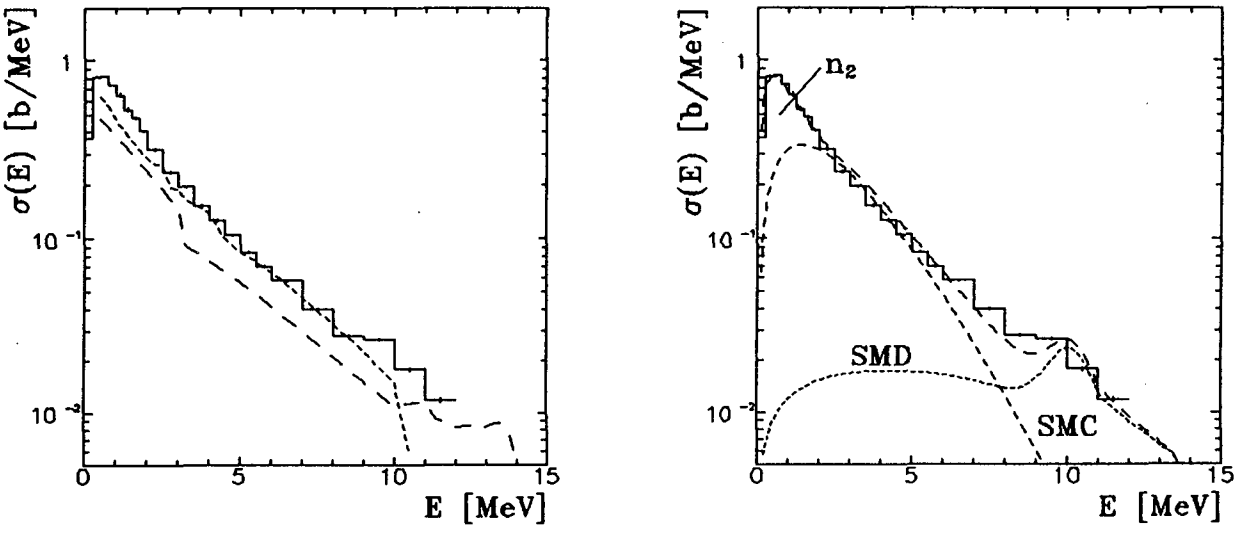

Fig. 2: Comparison of the evaluated experimental σ(E) (histogram) with ENDF/B-VI (short-dashed line) and ENDL-83 (dashed line) data, respectively (left hand), and with a SMD/SMC-model calculation (right hand)

[1)] Part of the IAEA Co-ordinated Research Programme (CRP) on "Measurement and Analysis of 14 MeV Neutron-Induced Double-Differential Neutron Emission Cross Sections needed for Fission and Fusion Reactor Technology"

References

[1] Nuclear Data for Fusion Reactor Technology, in Proc. Adv. Group Meeting of the IAEA, Gaussig 1986, IAEA-TECDOC-487, IAEA, Vienna, 1988

[2] H. Al Obiesi et al., in Proc. Int. Conf. on Nuclear Data for Science and Technology, 13 - 17 May 1991, Juelich

[3] A. Takahashi et al., OKTAVIAN-Report A-87-03, Osaka University (1987)

[4] M. Baba et al., JAERI-01-88-065, p. 365, Tokai, 1988

[5] H. Kalka, INDC(GDR)-059/L, IAEA, Vienna, 1990

3. A Benchmark for Iron Nuclear Data

T. Elfruth, K. Seidel, S. Unholzer

The shielding blanket of a fusion reactor must be optimized with respect to fast neutron flux, nuclear heating, and atomic displacements in the superconducting magnets. These parameters depend on the neutron and the gamma fluxes penetrating the shield. The uncertainties of the calculated values are dominated by the nuclear data uncertainties of Fe, with the largest contribution from neutron emission cross section uncertainties [1,2].

To gather information for a benchmark, a Fe slab assembly (100 cm * 100 cm * thickness D) was investigated by Monte Carlo calculations using the code MCNP and by some measurements. The block was bombarded with 14 MeV neutrons of a pulsed d-T neutron generator. A detector (liquid scintillator NE-213) was placed in a distance of about 3 m behind the slabs for the registration of

- proton-recoil spectra of the neutrons $\phi_n(E)$,
- Compton-electron spectra of the gammas $\phi_\gamma(E)$,
- time-of-arrival spectra of the neutrons and the gammas, $\phi_n(t)$ and $\phi_\gamma(t)$, respectively.

Fig.1 shows an example of the $\phi_n(t)$ calculated with the data of several libraries. $\phi_n(t)$ measured with an accuracy of $\approx$ 10 % can be used in a benchark. The comparison of a measured $\phi_n(t)$ with the calculated distribution allows to conclude that the main components of the experimental background are adequately taken into account.

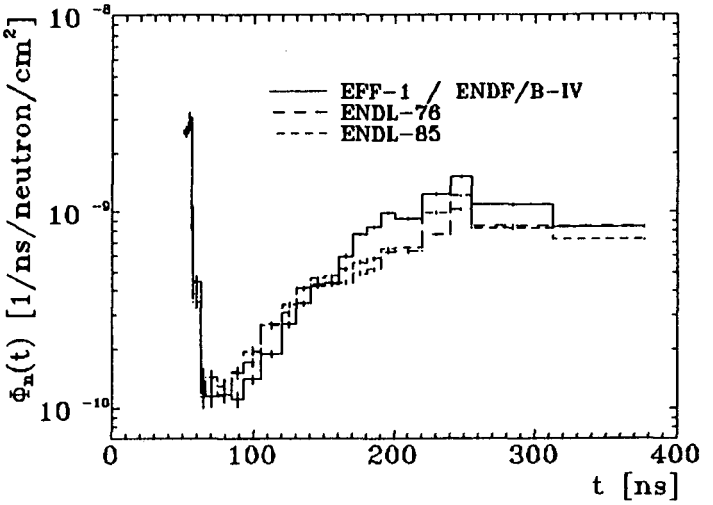

Fig. 1: Neutron time-of-arrival spectrum per one 14 MeV source neutron and per cm^2 at detector position for D = 30 cm calculated with the data of the libraries indicated.

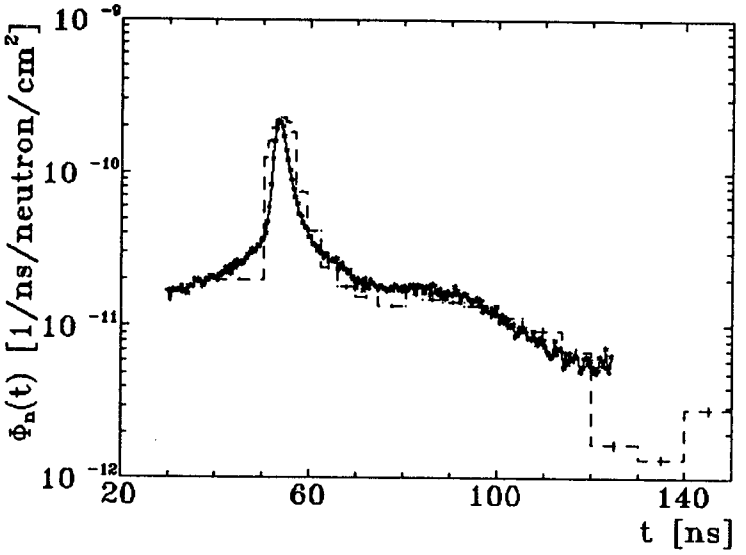

Fig. 2: Neutron time-of-arrival spectrum calculated with MCNP/EFF-1 (dashed histogram) and measured (•) with detector bias E_{eB} = 0.96 MeV for D = 32.5 cm.

References

[1] W. Daenner, ITER Expert Meeting on Shielding Experiments and Analysis, Garching (FRG), 1990

[2] T. Parish and A. Santamarina, Report CEA 91/333

4. Systematic Calculations of Fusion Activation Cross Sections using the EXIFON Computer Code

S. Eckstein, H. Kalka and D. Seeliger

The knowledge of a large number of neutron induced activation cross sections belongs to the most stringent nuclear data needs for fusion reactor safety calculations. The existing activation data libraries, however, show remarkable discrepancies even for many stable nuclei. Desired evaluated data for unstable nuclei do practically not exist at all. The aim of the present work was to compare the available evaluations ADL-90, HEDL, ECN, B86, and SINCROSACT with model calculations using the statistical multistep code EXIFON [1-3], to get an independent information in support of one or the other set of evaluated excitation functions.

Calculations of the (n,p)-, (n,2n)-, and (n,α)-cross sections were performed using "global" model parameters [1], without any fitting procedure. In this way, cross sections from threshold up to 25 MeV incidence energy were reasonably reproduced for the following nuclei:

^{24}Mg, ^{34}S, ^{35}Cl, ^{40}Ca, ^{42}Ca, ^{44}Ca, ^{45}Ca, ^{45}Sc, ^{50}Cr, ^{52}Cr, ^{55}Mn, ^{56}Fe, ^{58}Ni, ^{60}Ni, ^{64}Ni, ^{92}Mo, ^{92}Nb, ^{93}Nb, ^{94}Mo, ^{95}Nb, ^{99}Mo, ^{100}Mo, ^{107}Ag, ^{109}Ag, ^{112}Sn, ^{116}Sn, ^{123}Sn, ^{137}Ba, ^{140}Ce, ^{142}Ce, ^{150}Nd, ^{151}Eu, ^{165}Ho, ^{179}Hf, ^{180}Hf, ^{187}Re, ^{192}Os, ^{195}Hg, ^{197}Hg, ^{204}Pb, ^{206}Pb, ^{208}Bi, ^{210}Po.

A typical example is shown on fig.1. In a few cases, reasonable agreement with experimental data could only be obtained by modifying the effective pairing energy (i.e. changing the effective residual interaction energy): ^{39}K, ^{41}K, ^{63}Ni, ^{63}Cu, ^{93}Nb.

The present study shows that by the use of the EXIFON computer code a bulk of the activation cross sections of interest (in the order of 10^4 c.s.!) can be calculated with reasonable accuracy in a short time. (Note that the calculation of an excitation function having 25 data points takes about 3 min with IBM PC 486, only.)

References

[1] H. Kalka, in "Nuclear Reaction Mechanismus", ed. by D. Seeliger and H. Kalka, World Scientific Publ. Comp., Singapore (1991) 87

[2] H. Kalka, M. Torjman, D. Seeliger, Phys. Rev. **C40** (1989) 1619

[3] H. Kalka, M. Torjman, H. N. Lien, R. Lopez, D. Seeliger, Z. Phys. **A335** (1990) 163

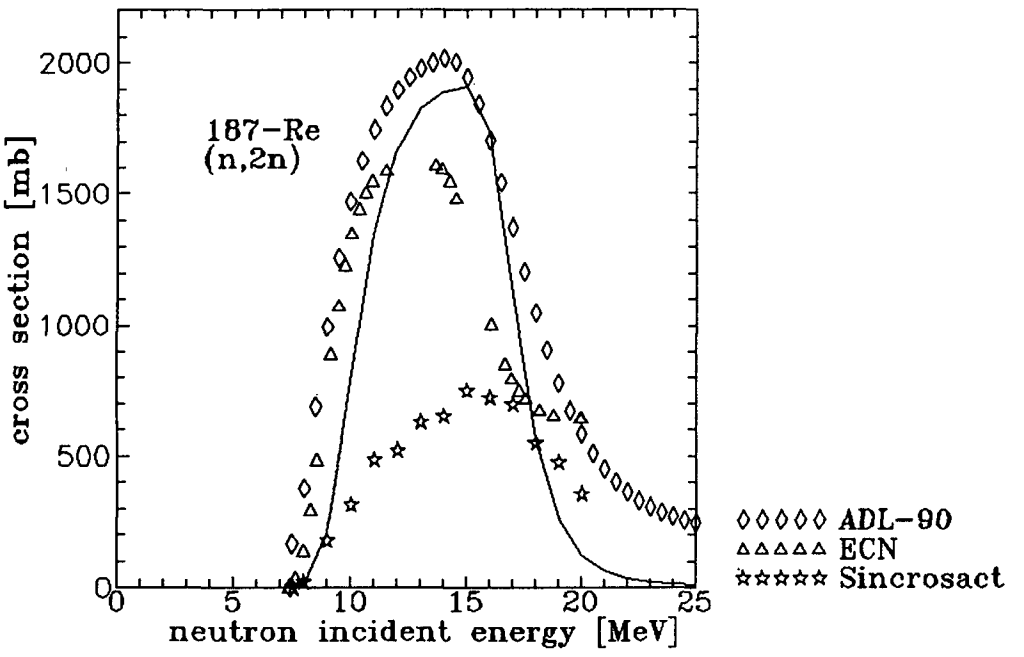

Fig. 1 Comparison between the calculated (n,2n) cross section for ^{187}Re with three evaluated libraries ADL-90, ECN and SINCROSACT. The model curve is given by the solid line.

5. Data Files for X-Ray Emission Rates and Intensity Ratios

K.Sieber, I.Reiche, G.Zschornack

For a wide field of applications and for fundamental research X-ray emission rates and also intensity ratios are neccessary for different elements and transitions. Experimental results about this quantities one can only get for intensity ratios, which are simultaneously a proof of the accuracy for calculated emission rates. Since there is an increasing need for very accurate, evaluated data we have started to create files with the above mentioned data for neutral and ionized atoms under the data bank program dBASE. For X-ray emission rates there are included calculated data from different approximation levels. An overview about calculation methods for X-ray emission data gives Reiche [RE92]. Up to now we have included at about 5000 emission rates in the data files. These data are mostly related to neutral atoms; calculated values for ionized atoms we will include in a next step.

For intensity ratios also more than 5000 values are fixed from calculated emission data as well as from experimental investigations. There are collected data up to 1991 from standard publications but also from various publications containing only a small number of data for selected elements. Further activities are neccessary to complete the data for the period between 1920 and 1950 and for the years after 1980.

As an instance for graphical representation of the collected data in Fig.1 K_β/K_α emission rates are shown for the atomic numbers less then 40. This region was choosen because here are the most interesting deviations between experimental data and results from different approximation levels.

References

[RE92] I.Reiche; Doctor Thesis, TU Dresden, Dresden, 1992

[HN70] J.S.Hansen et al.; Nucl.Physics A142 (1970) 604

[MI71] V.D.Mistry et al.; Nucl.Physics A164 (1971) 219

[PA76] G.Paig et al.; Phys.Review A14 (1976) 2190

[PE76] G.Paig et al.; Phys.Review A14 (1976) 2190

[PE87] A.Perujo et al.; J.Phys. B20 (1987) 5647

[RE91] I.Reiche; unpublished results

[SA74] S.I.Salem et al.; At.Data Nucl.Data Tables 14 (1974) 91

[SL72] V.W.Slivinsky et al.; Phys.Review A5 (1972) 1581

[SO74] J.H.Scofield; Phys.Review A9 (1974) 1041

[VE86] N.Venkateswara Rao et al.; Physica 138C (1986) 215

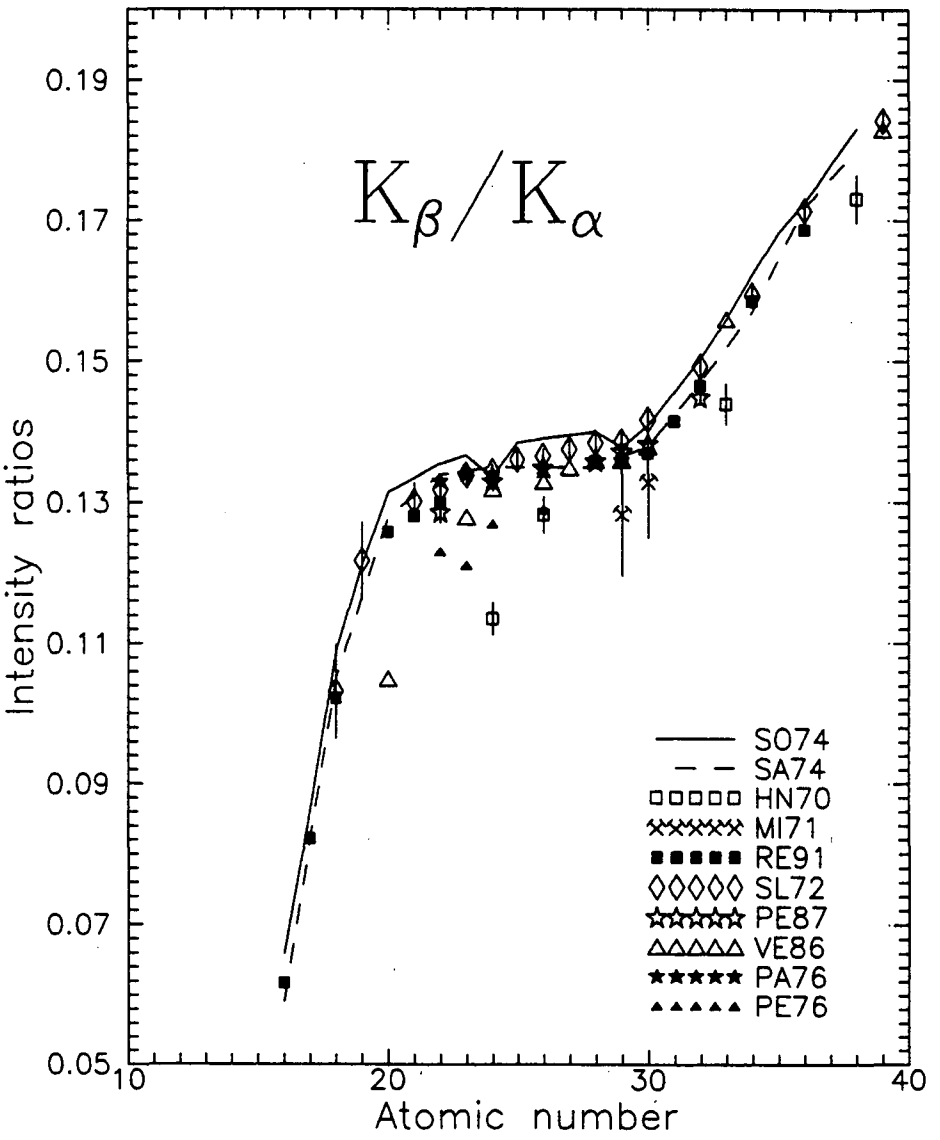

Figure 1: K_β/K_α intensity ratios as a function of the atomic number Z.

6. Systemization of X-Ray Transition Energies

K.Sieber, I.Reiche, G.Zschornack

Various applications of XRF and accelerator-based PIXE and HIXE measurements demand precision atomic data from neutral free atoms or from chemical compounds. Other fields of basic research, such as fusion research or the development of sources of coherent light, require considerable information about atomic data from ionized species. For many purposes it is difficult to rapidly find all atomic data in a useable form. Therefore, we have started activities to create atomic data files of neutral and ionized atoms.

The data files contain both experimental values and calculated ones. Up to now we have included at about 4700 values for neutral atoms from different sources. The data are stored together with their actual reference, their experimental errors and with short remarks about the method of measurement or the calculation method, respectively. For atomic ground states about 30000 data of X-ray energy shifts, calculated with the Dirac-Fock-Slater method are also available. As a next step the data files should be extended to experimental transition energies from ionized atoms.

All data are stored in dBASE IV. This system allows several data manipulations for creation of special files for selected data groups, their graphical representation and evaluation.

For instance, in Fig.1 relative deviations of experimentally measured K_{α_1} X-ray energies as a function of the atomic number Z are compared. As reference data experimental ones from Bearden [BA67] are taken. The graphical representation shows the confidence limits of the atomic data used and any inconsistencies between these datas.

References

[BA67] J.A.Bearden; Rev.Mod.Physics 39 (1967) 78

[CA78] Y.Cauchois et al.; Int.Tables of Selected Constants, Vol.18, 1978

[CA89] J.L.Campbell et al.; At.Data Nucl.Data Tables 43 (1989) 281

[DE79] R.D.Deslattes et al.; Phys.Letters 71A (1979) 411

[DI71] P.F.Dittner et al.; Phys.Rev.Letters 26 (1971) 1037

[DI72] P.F.Dittner et al.; Phys.Review A5 (1972) 481

[KE82] E.G.Kessler Jr. et al.; Phys.Review A26 (1982) 2696

[SI92] K.Sieber; Diploma Thesis, TU Dresden, Institute for Nuclear and Atomic Physics, Dresden, 1992

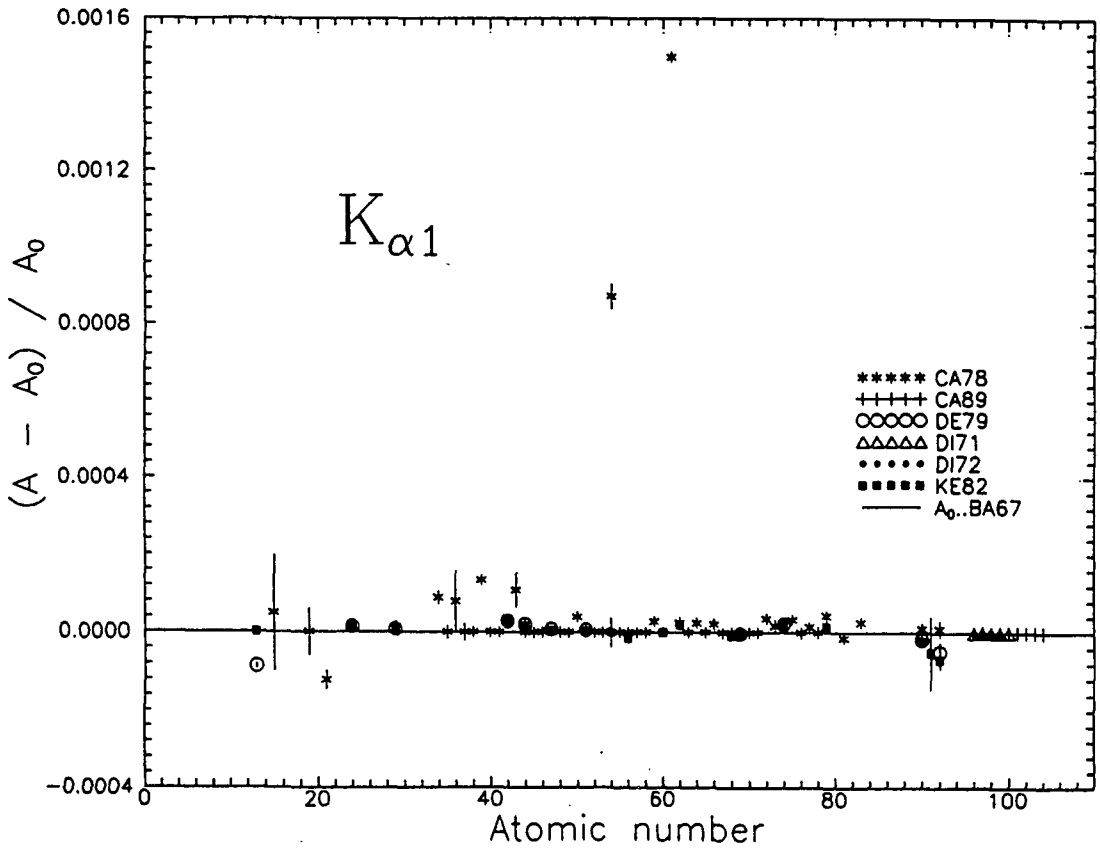

Figure 1: Relative deviations $(A-A_0)/A_0$ of experimentally measured K_{α_1} X-ray transition energy data as a function of atomic number Z.

ABTEILUNG NUKLEARCHEMIE
UNIVERSITÄT ZU KÖLN
AND
ZENTRALEINRICHTUNG FÜR STRAHLENSCHUTZ
UNIVERSITÄT HANNOVER

1. Proton-Induced Spallation at 1600 MeV

M. Lüpke[1], H.-J. Lange[1], M. Schnatz-Büttgen[1], R. Michel[1], R. Rösel[2], U. Herpers[2], P. Cloth[3], D. Filges[3]

During recent years our collaboration made comprehensive investigations of residual nuclide production by p-induced reactions for energies between 600 MeV and 2.6 GeV [1-7]. These investigations were aimed to a better understanding of medium energy reactions and to improve the cross section data base needed for model calculations of the production of cosmogenic nuclides in terrestrial and extraterrestrial matter [8]. In the last year this work was continued by measurements of spallation cross sections for an energy of 1.6 GeV. Thin stacks of pure element foils, technical alloys and suitable chemical compounds were irradiated with 1.6 GeV protons at the Saturne accelerator of the Laboratoire National Saturne, Saclay/France.

The target elements cover C, N, O, Mg, Al, Si, Ca, Ti, Mn, Fe, Co, Ni, Cu, Rb, Sr, Y, Zr, Rh, Ba, and Au. The produced radionuclides were measured by gamma-spectrometry. Gamma-energies, branching ratios and half-lifes of the radionuclides, which were used for the calculation of cross sections, were taken from [9,10]. The proton fluxes were determined on the basis of the cross sections for the reaction $^{27}Al(p,3p3n)^{22}Na$ as recommended by Tobailem and de Lassus St. Genies [11]. The actual cross section adopted for this reaction was 13.22 mb. A detailed discussion of the errors of cross section determination is given elsewhere [2,4]. The data evaluation for the target elements Ba and Au is not yet finished. Measurements of longlived radionuclides and stable rare gas isotopes by accelerator and conventional mass spectrometry are still going on.

1 Zentraleinrichtung für Strahlenschutz, Universität Hannover, F.R.G.
2 Abteilung Nuklearchemie, Universität zu Köln, F.R.G.
3 Arbeitsgruppe Strahlungstransport, IKP/KFA Jülich, F.R.G.

A detailed analysis of possible interferences from secondary protons and neutrons was performed on the basis of secondary particle spectra calculated by Monte Carlo techniques using the HERMES code system [12]. These spectra and a set of experimental and theoretical excitation functions for p- and n-induced reaction, which was validated by thick-target simulation experiments [13,14], allowed to correct the experimental cross sections for the contribution of residual nuclide production by secondary particles. In table 1 the results are presented for target elements from oxygen to rhodium.

An equivalent analysis of our earlier data for energies of 800 MeV, 1.2 GeV and 2.6 GeV is presently performed. A compilation of all results for energies between 800 MeV and 2.6 GeV will soon be published. Together with the data for proton energies up to 200 MeV measured earlier by our group [15,16, and references therein] they give fairly complete excitation functions from the thresholds up to 2600 MeV.

References

[1] R. Michel, P. Dragovitsch, K. Prescher, M.N. Rao, J. Methew, in: Progress Report on Nuclear Data Research in the Federal Republic of Germany for the Period April, 1st, 1987 to March, 31th, 1988, NEANDC(E)-292 U Vol. V INDC(Ger)-32/LN+Special, 1988, 25.

[2] R. Michel, B. Dittrich, U. Herpers, T.Schiffmann, P. Cloth, P. Dragovitsch, D. Filges, The Analyst 114 (1989) 287.

[3] B. Dittrich, U. Herpers, M. Lüpke, R. Michel, in: Progress Report on Nuclear Data Research in the Federal Republic of Germany for the Period April, 1st, 1988 to March, 31th, 1989, NEANDC(E)-292 U Vol. V INDC(Ger)-34/LN+Special (1989) 31.

[4] B. Dittrich, U. Herpers, M. Lüpke, R. Michel, H.J. Hofmann, W. Wölfli, Radiochimica Acta 50 (1990) 11.

[5] B. Dittrich, U. Herpers, H.J. Hofmann, W. Wölfli, R. Bodemann, M. Lüpke, R. Michel, P. Dragovitsch, D. Filges, Nucl. Instr. Meth. Phys. Res. B52 (1990) 588.

[6] B. Dittrich, U. Herpers, R. Bodemann, M. Lüpke, R. Michel, P. Signer, R. Wieler, H.J. Hofmann, W. Wölfli, in: Progress Report on Nuclear Data Research in the Federal Republic of Germany for the Period April, 1st, 1989 to March, 31th, 1990, NEANDC(E)-312-U Vol. V INDC(Ger)-35/LN + Special, 1990, 45.

[7] M. Lüpke, R. Michel, B. Dittrich, U. Herpers,P. Dragovitsch, D. Filges, H.J. Hofmann, W. Wölfli, Proc. Int. Conf. "Nuclear Data for Science and Technology", Jülich 13 - 17 Mai, 1991, in press.

[8] R. Michel, in: N.P. Kocherov, Intermediate Energy Nuclear Data for Applications, INDC(NDS)-245 (1991) 17, IAEA, Wien.

[9] W. Seelmann-Eggebert, G. Pfennig, H. Muenzel, H. Kleve-Nebenius, Chart of the Nuclides, 5th Edition, Kommunalschriften-Verlag Jehle, Muenchen (1981).

[10] U. Reuss, W. Westmeier, Atomic Data Nucl. Data Tables 29 (1983) 1 and ibid. 193.

[11] J. Tobailem, C.H. de Lassus St. Genies, Additif No. 2 a la CEA-N-1466(1) (1975), CEA-N-1466(5) (1981).

[12] P. Cloth, D. Filges, R.D. Neef, G. Sterzenbach, C. Reul, T.W. Armstrong, B.L. Colborn, Juel-2203 (1988).

[13] R. Michel, F. Peiffer, S. Theis, F. Begemann, H. Weber, P. Signer, R. Wieler, P. Cloth, P. Dragovitsch, D. Filges, P. Englert, Nucl. Instr. Meth. Phys. Res. B42 (1989) 76.

[14] R. Michel, M. Lüpke, U. Herpers, D. Filges, P. Dragovitsch, W. Wölfli, B. Dittrich, H.J. Hofmann, Proc. 8th Int. Conf. Modern Trends in Activation Analysis, Vienna, Sept. 16 - 20, 1991, J. Radioanal. Nuclear Chem., submitted.

[15] B. Dittrich, U. Herpers, R. Bodemann, R. Michel, H. Condé, B. Holmqvist, P. Malmborg, in: Progress Report on Nuclear Data Research in the Federal Republic of Germany for the Period April, 1st, 1989 to March, 31th, 1990, NEANDC(E)-312-U Vol. V INDC(Ger)-35/LN + Special, 1990, 57 - 61.

[16] R. Bodemann, R. Michel, B. Dittrich, U. Herpers, R. Rösel, H.J. Hofmann, W. Wölfli, B. Holmqvist, H. Condé, P. Malmborg, Proc. Int. Conf. "Nuclear Data for Science and Technology", Jülich 13 - 17 Mai, 1991, in press.

Table 1: Cross sections for the production of radionuclides by 1.6 GeV protons from target elements C, N, O, Mg, Al, Si, Ca, Ti, Mn, Fe, Co, Ni, Cu, Rb, Sr, Y, Zr, and Rh (continued).

REACTION	CROSS SECTION [mb]	REACTION	CROSS SECTION [mb]
$Fe(p,Xn)^{58}Co$	0.113 ± 0.015	$Ni(p,2pXn)^{56}Co$	31.7 ± 2.8
		$Ni(p,2pXn)^{57}Co$	55.3 ± 5.7
$Co(p,24p29n)^{7}Be$	6.34 ± 0.51	$Ni(p,2pXn)^{58}Co$	6.66 ± 0.95
$Co(p,17p21n)^{22}Na$	1.74 ± 0.14	$Ni(p,2pXn)^{60}Co$	1.10 ± 0.14
$Co(p,17p19n)^{24}Na$	2.93 ± 0.23	$Ni(p,pXn)^{56}Ni$	2.24 ± 0.21
$Co(p,9p9n)^{42}K$	5.42 ± 0.44	$Ni(p,pXn)^{57}Ni$	20.0 ± 1.8
$Co(p,9p8n)^{43}K$	1.86 ± 0.14		
$Co(p,7p9n)^{44m}Sc$	7.72 ± 0.60	$Cu(p,26pXn)^{7}Be$	6.34 ± 0.51
$Co(p,7p7n)^{46}Sc$	9.23 ± 0.71	$Cu(p,19pXn)^{22}Na$	1.36 ± 0.12
$Co(p,7p6n)^{47}Sc$	3.79 ± 0.29	$Cu(p,19pXn)^{24}Na$	2.56 ± 0.20
$Co(p,7p5n)^{48}Sc$	0.148 ± 0.021	$Cu(p,18pXn)^{28}Mg$	0.331 ± 0.048
$Co(p,5p7n)^{48}V$	13.8 ± 1.1	$Cu(p,11pXn)^{42}K$	4.62 ± 0.46
$Co(p,4p8n)^{48}Cr$	0.419 ± 0.037	$Cu(p,11pXn)^{43}K$	1.72 ± 0.14
$Co(p,4p5n)^{51}Cr$	28.4 ± 2.3	$Cu(p,10pXn)^{47}Ca$	0.085 ± 0.013
$Co(p,3p5n)^{52}Mn$	7.98 ± 0.64	$Cu(p,9pXn)^{44m}Sc$	6.89 ± 0.55
$Co(p,3p3n)^{54}Mn$	28.1 ± 2.3	$Cu(p,9pXn)^{46}Sc$	7.99 ± 0.65
$Co(p,p3n)^{56}Co$	5.95 ± 0.55	$Cu(p,9pXn)^{47}Sc$	2.60 ± 0.27
$Co(p,p2n)^{57}Co$	24.6 ± 2.3	$Cu(p,7pXn)^{48}V$	11.8 ± 1.0
$Co(p,pn)^{58}Co$	32.7 ± 3.7	$Cu(p,6pXn)^{48}Cr$	0.405 ± 0.036
$Co(p,4n)^{56}Ni$	0.398 ± 0.150	$Cu(p,6pXn)^{51}Cr$	24.3 ± 2.0
$Co(p,3n)^{57}Ni$	0.109 ± 0.015	$Cu(p,5pXn)^{52}Mn$	7.52 ± 0.62
		$Cu(p,5pXn)^{54}Mn$	19.3 ± 1.6
$Ni(p,25pXn)^{7}Be$	8.81 ± 0.73	$Cu(p,4pXn)^{59}Fe$	1.81 ± 0.17
$Ni(p,18pXn)^{22}Na$	2.43 ± 0.20	$Cu(p,3pXn)^{56}Co$	7.49 ± 0.64
$Ni(p,18pXn)^{24}Na$	2.48 ± 0.22	$Cu(p,3pXn)^{57}Co$	21.4 ± 1.9
$Ni(p,10pXn)^{42}K$	2.67 ± 0.31	$Cu(p,3pXn)^{58}Co$	28.4 ± 2.5
$Ni(p,10pXn)^{43}K$	0.781 ± 0.071	$Cu(p,3pXn)^{60}Co$	9.28 ± 0.89
$Ni(p,8pXn)^{44m}Sc$	8.68 ± 0.69	$Cu(p,2pXn)^{56}Ni$	0.413 ± 0.134
$Ni(p,8pXn)^{46}Sc$	5.46 ± 0.43	$Cu(p,2pXn)^{57}Ni$	0.902 ± 0.083
$Ni(p,8pXn)^{47}Sc$	0.878 ± 0.170	$Cu(p,Xn)^{62}Zn$	0.433 ± 0.063
$Ni(p,6pXn)^{48}V$	19.7 ± 1.6	$Cu(p,Xn)^{65}Zn$	0.299 ± 0.044
$Ni(p,5pXn)^{48}Cr$	1.70 ± 0.14		
$Ni(p,5pXn)^{51}Cr$	34.6 ± 2.8	$Rb(p,17pXn)^{46}Sc$	5.52 ± 0.56
$Ni(p,4pXn)^{52}Mn$	12.3 ± 1.0	$Rb(p,14pXn)^{51}Cr$	8.28 ± 3.20
$Ni(p,4pXn)^{54}Mn$	13.8 ± 1.2	$Rb(p,13pXn)^{54}Mn$	15.2 ± 1.6
$Ni(p,3pXn)^{59}Fe$	0.268 ± 0.037	$Rb(p,12pXn)^{59}Fe$	2.55 ± 0.28

Table 1: Cross sections for the production of radionuclides by 1.6 GeV protons from target elements C, N, O, Mg, Al, Si, Ca, Ti, Mn, Fe, Co, Ni, Cu, Rb, Sr, Y, Zr, and Rh (continued).

REACTION	CROSS SECTION [mb]	REACTION	CROSS SECTION [mb]
$Rb(p,11pXn)^{56}Co$	3.84 ± 0.40	$Y(p,36p47n)^{7}Be$	6.47 ± 0.63
$Rb(p,11pXn)^{58}Co$	20.0 ± 2.0	$Y(p,29p37n)^{24}Na$	1.07 ± 0.13
$Rb(p,11pXn)^{60}Co$	8.66 ± 0.91	$Y(p,17p25n)^{48}V$	2.89 ± 0.21
$Rb(p,8pXn)^{65}Zn$	27.3 ± 3.0	$Y(p,15p23n)^{52}Mn$	2.50 ± 0.18
$Rb(p,4pXn)^{75}Se$	42.0 ± 4.3	$Y(p,14p17n)^{59}Fe$	0.924 ± 0.096
$Rb(p,pXn)^{83}Rb$	73.7 ± 7.7	$Y(p,13p21n)^{56}Co$	2.36 ± 0.18
$Rb(p,pXn)^{84}Rb$	73.2 ± 8.6	$Y(p,13p19n)^{58}Co$	10.2 ± 0.8
		$Y(p,13p17n)^{60}Co$	4.29 ± 0.71
$Sr(p,28pXn)^{22}Na$	0.585 ± 0.067	$Y(p,10p15n)^{65}Zn$	17.2 ± 1.3
$Sr(p,18pXn)^{46}Sc$	2.82 ± 0.33	$Y(p,9p14n)^{67}Ga$	18.3 ± 1.3
$Sr(p,16pXn)^{48}V$	2.94 ± 0.32	$Y(p,8p13n)^{69}Ge$	11.3 ± 0.8
$Sr(p,15pXn)^{51}Cr$	7.62 ± 0.85	$Y(p,7p12n)^{71}As$	16.2 ± 1.2
$Sr(p,14pXn)^{52}Mn$	2.50 ± 0.30	$Y(p,7p9n)^{74}As$	6.75 ± 0.50
$Sr(p,14pXn)^{54}Mn$	8.65 ± 1.11	$Y(p,6p9n)^{75}Se$	26.2 ± 1.9
$Sr(p,13pXn)^{59}Fe$	1.39 ± 0.15	$Y(p,3p4n)^{83}Rb$	51.8 ± 3.8
$Sr(p,12pXn)^{56}Co$	2.28 ± 0.27	$Y(p,3p3n)^{84}Rb$	14.9 ± 1.2
$Sr(p,12pXn)^{58}Co$	11.6 ± 1.2	$Y(p,2p5n)^{83}Sr$	24.9 ± 1.9
$Sr(p,12pXn)^{60}Co$	3.98 ± 0.49	$Y(p,pn)^{88}Y$	29.6 ± 3.8
$Sr(p,11pXn)^{56}Ni$	1.56 ± 0.23	$Y(p,2n)^{88}Zr$	1.41 ± 0.20
$Sr(p,10pXn)^{67}Cu$	6.53 ± 0.72	$Y(p,n)^{89}Zr$	0.635 ± 0.094
$Sr(p,8pXn)^{67}Ga$	16.2 ± 1.8		
$Sr(p,7pXn)^{69}Ge$	10.5 ± 1.2	$Zr(p,37pXn)^{7}Be$	5.65 ± 0.53
$Sr(p,6pXn)^{71}As$	12.9 ± 1.4	$Zr(p,20pXn)^{46}Sc$	2.03 ± 0.17
$Sr(p,6pXn)^{72}As$	19.4 ± 2.1	$Zr(p,18pXn)^{48}V$	2.87 ± 0.25
$Sr(p,6pXn)^{74}As$	9.15 ± 0.97	$Zr(p,17pXn)^{51}Cr$	5.83 ± 0.55
$Sr(p,6pXn)^{76}As$	28.7 ± 3.5	$Zr(p,16pXn)^{52}Mn$	2.24 ± 0.19
$Sr(p,5pXn)^{75}Se$	24.5 ± 2.7	$Zr(p,15pXn)^{59}Fe$	0.853 ± 0.082
$Sr(p,4pXn)^{77}Br$	53.4 ± 6.3	$Zr(p,14pXn)^{56}Co$	2.33 ± 0.44
$Sr(p,4pXn)^{82}Br$	3.60 ± 0.40	$Zr(p,9pXn)^{69}Ge$	10.6 ± 0.9
$Sr(p,2pXn)^{83}Rb$	43.7 ± 4.8	$Zr(p,8pXn)^{71}As$	14.6 ± 1.2
$Sr(p,2pXn)^{84}Rb$	25.4 ± 2.8	$Zr(p,8pXn)^{74}As$	5.44 ± 0.45
$Sr(p,pXn)^{83}Sr$	12.9 ± 1.5	$Zr(p,7pXn)^{75}Se$	23.2 ± 1.9
$Sr(p,pXn)^{85}Sr$	12.5 ± 2.1	$Zr(p,4pXn)^{83}Rb$	37.1 ± 3.2
$Sr(p,Xn)^{87}Y$	8.25 ± 0.89	$Zr(p,4pXn)^{84}Rb$	7.11 ± 0.63
$Sr(p,Xn)^{87m}Y$	11.3 ± 1.6	$Zr(p,3pXn)^{83}Sr$	19.4 ± 1.7
$Sr(p,Xn)^{88}Y$	4.83 ± 0.51	$Zr(p,2pXn)^{87}Y$	41.4 ± 4.1

Table 1: Cross sections for the production of radionuclides by 1.6 GeV protons from target elements C, N, O, Mg, Al, Si, Ca, Ti, Mn, Fe, Co, Ni, Cu, Rb, Sr, Y, Zr, and Rh (continued).

REACTION	CROSS SECTION [mb]	REACTION	CROSS SECTION [mb]
$Zr(p,2pXn)^{88}Y$	22.9 ± 2.4	$Rh(p,10p15n)^{79}Kr$	18.5 ± 1.7
$Zr(p,pXn)^{88}Zr$	22.5 ± 2.4	$Rh(p,9p12n)^{83}Rb$	30.1 ± 2.5
$Zr(p,pXn)^{89}Zr$	25.6 ± 3.0	$Rh(p,9p11n)^{84}Rb$	2.91 ± 0.24
$Zr(p,pXn)^{95}Zr$	0.809 ± 0.112	$Rh(p,8p14n)^{82}Sr$	14.6 ± 1.2
		$Rh(p,7p10n)^{87}Y$	36.1 ± 3.0
$Rh(p,35p47n)^{22}Na$	0.410 ± 0.066	$Rh(p,7p6n)^{91}Y$	18.1 ± 5.2
$Rh(p,25p33n)^{46}Sc$	0.985 ± 0.084	$Rh(p,6p12n)^{86}Zr$	8.35 ± 0.74
$Rh(p,23p33n)^{48}V$	1.16 ± 0.10	$Rh(p,6p10n)^{88}Zr$	28.7 ± 2.4
$Rh(p,21p31n)^{52}Mn$	1.01 ± 0.10	$Rh(p,6p9n)^{89}Zr$	33.0 ± 2.8
$Rh(p,20p25n)^{59}Fe$	0.416 ± 0.048	$Rh(p,6pn)^{97}Zr$	1.49 ± 0.20
$Rh(p,19p29n)^{56}Co$	0.993 ± 0.085	$Rh(p,5p9n)^{90}Nb$	32.3 ± 2.7
$Rh(p,19p27n)^{58}Co$	4.73 ± 0.39	$Rh(p,5p8n)^{91m}Nb$	1.32 ± 0.38
$Rh(p,19p25n)^{60}Co$	2.14 ± 0.20	$Rh(p,5p7n)^{92m}Nb$	2.00 ± 0.18
$Rh(p,16p23n)^{65}Zn$	9.58 ± 0.80	$Rh(p,3p6n)^{95m}Tc$	2.92 ± 0.26
$Rh(p,14p22n)^{68}Ge$	6.77 ± 0.95	$Rh(p,3p5n)^{96}Tc$	19.6 ± 1.7
$Rh(p,13p20n)^{71}As$	10.4 ± 0.9	$Rh(p,2p5n)^{97}Ru$	27.5 ± 2.5
$Rh(p,13p17n)^{74}As$	3.67 ± 0.30	$Rh(p,p2n)^{101}Rh$	1.86 ± 0.28
$Rh(p,12p19n)^{73}Se$	11.1 ± 1.3	$Rh(p,p2n)^{101m}Rh$	9.64 ± 1.28
$Rh(p,12p17n)^{75}Se$	19.4 ± 1.6	$Rh(p,pn)^{102m}Rh$	31.4 ± 3.4

INSTITUT FÜR KERNCHEMIE
PHILLIPPS-UNIVERSITÄT MARBURG

New Measurement of ^{234m}Pa Gamma-Ray Intensities Following the Decay of ^{238}U §

K. Siemon, R.A. Esterlund, J. van Aarle, M. Knaack, W. Westmeier and P. Patzelt

In such diverse scientific and technological areas as environmental studies, radiation protection and nuclear-fuel reprocessing, the determination of the ^{238}U content of a sample is often of paramount interest. In comparison with many chemical methods and alpha-particle spectrometry, however, the quantitative assay of ^{238}U via gamma-ray spectrometry offers the considerable advantage of simplified sample preparation. A necessary condition for the viability of this method is that the absolute intensities I_γ of the gamma-rays utilized in the determination of the ^{238}U content be known both accurately and with sufficient precision.

The method of determining the ^{238}U content of a sample by gamma-ray spectrometry of ^{235}U and its decay products followed by deduction of the ^{238}U content from the known isotopic ratios is only reliable when it is known with certainty that no physical process has occurred which would fractionate these ratios. The alternative use of the gamma lines of decay-chain products from ^{234}U for ^{238}U assay in a given sample is reliable only when it is known with certainty that no chemical processes have occurred during the history of the sample which might perturb the secular equilibrium between ^{238}U and the decay-chain products of ^{234}U. As secular equilibrium between ^{238}U and ^{234m}Pa is relatively quickly attained, the 1001-keV gamma line of ^{234m}Pa would seem to be highly suitable for assay of ^{238}U.

Gamma-ray lines following the decay of ^{234m}Pa were assayed via high-purity germanium-crystal (HPGe) spectrometry of analytical-grade foils of depleted uranium metal. Absolute intensities were determined for the 42 strongest lines ($I_\gamma \geq 0.002\%$), with special emphasis on the 1001-keV line, which is often used for either assay or normalization purposes. The I_γ value derived for this latter line was independently confirmed in two further measurements, in which its intensity relative to the 185.7-keV gamma line which accompanies the decay of ^{235}U was compared. Our new value for the absolute intensity of this line I_γ (1001 keV) is (0.845 ± 0.021)%, which is over 1.4 times greater than the currently-accepted value.

Intensity of the 1001-keV line of ^{234m}Pa : I_γ = 0.845 % ± 0.021 %

Further gamma-ray transitions (x 10^5) of ^{234m}Pa with $I_\gamma \geq 0.03$ % :

E_γ (keV)	I_γ	ΔI_γ
766.3	317.57	9.00
742.7	87.85	4.21
258.3	72.59	4.75
786.2	50.44	2.79

§ To be published in Int. J. Appl. Radiat. Isot. **43** (1992).

PHYSIKALISCH TECHNISCHE BUNDESANSTALT BRAUNSCHWEIG

1. Neutron Data

1.1 Cross Sections for the $^{56}Fe(n,p)^{56}Mn$ Reaction

W. Mannhart, G.Börker

In addition to the measurement of the cross sections of $^{54}Fe(n,\alpha)^{51}Cr$ and $^{54}Fe(n,p)^{54}Mn$ already reported elsewhere [1], measurements of the cross section for the $^{56}Fe(n,p)^{54}Mn$ reaction were carried out in the neutron energy range between 9.1 and 14.6 MeV. As in the previous experiment, neutrons were produced via the $D(d,n)^3He$ reaction and the neutron fluence was monitored with the $^{27}Al(n,\alpha)^{24}Na$ reaction. Careful corrections were applied for complementary neutrons from the D(d,np) breakup reaction and for neutrons scattered from the support structures into the iron samples. Final uncertainties between 2.8% and 4.2% were achieved in the experiment. In Fig. 1 the data of the present work are compared with

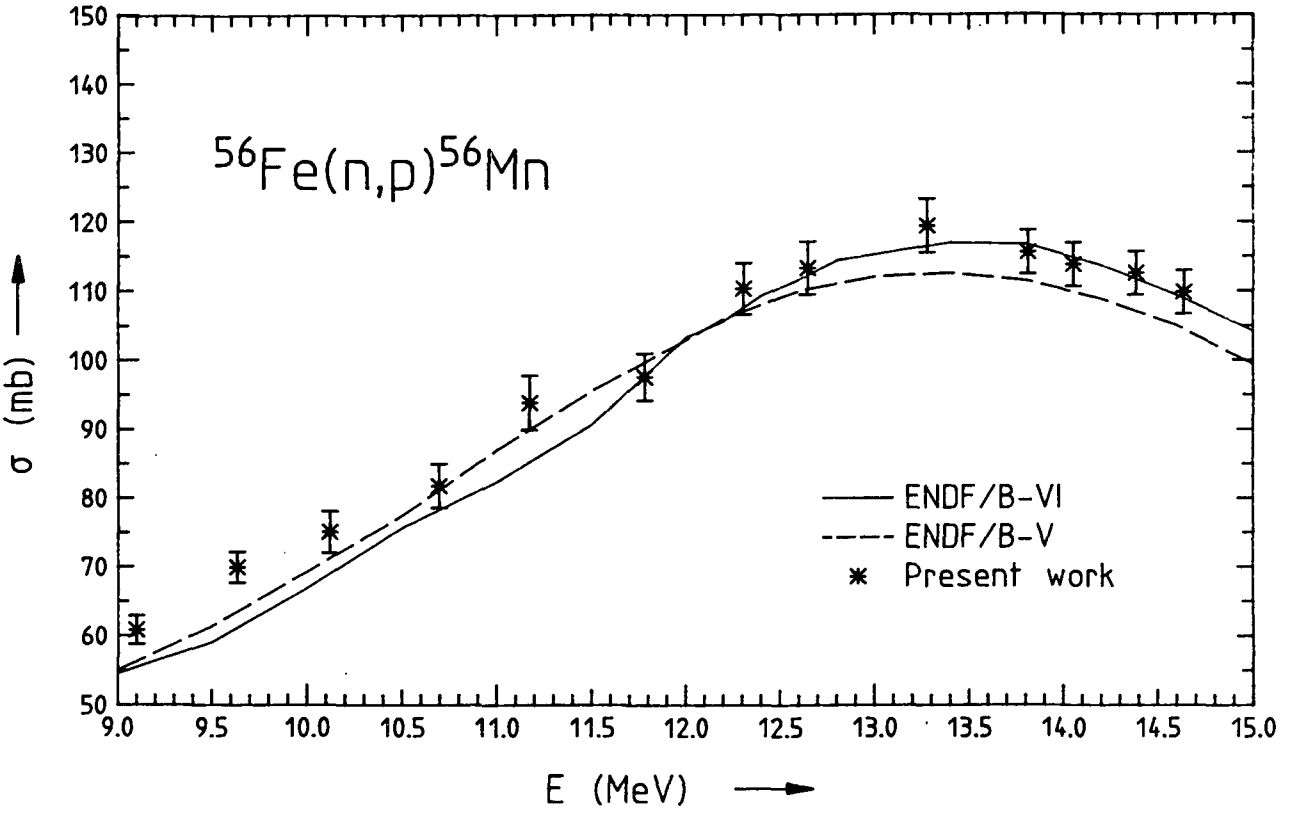

Fig. 1 Cross section data for the $^{56}Fe(n,p)^{56}Mn$ reaction and comparison with the ENDF/B-V and ENDF/B-VI evaluations

the ENDF/B-V and ENDF/B-VI evaluations. Our data are highly consistent with a recent evaluation of 14 MeV data [2]. The difference between our data and the data from this evaluation amounts to 0.6%.

1.2 Cross Sections for the $^{93}Nb(n,2n)^{92m}Nb$ Reaction

W. Mannhart, D. Schmidt, R. Nolte

In a recent intercomparison of activation cross-section measurements the $^{58}Ni(n,p)^{58}Co$ and $^{93}Nb(n,2n)^{92m}Nb$ reactions have been investigated [3]. The result of the $^{93}Nb(n,2n)^{92m}Nb$ reaction is almost exclusively based on an experiment performed at PTB. In this experiment a deuterium gas target was used to generate neutrons between 9.1 and 13.5 MeV with the $D(d,n)^3He$ reaction. Metallic samples of niobium were irradiated at zero degrees at a distance of 10 cm from the target. The samples were attached to a low-mass fission chamber with a

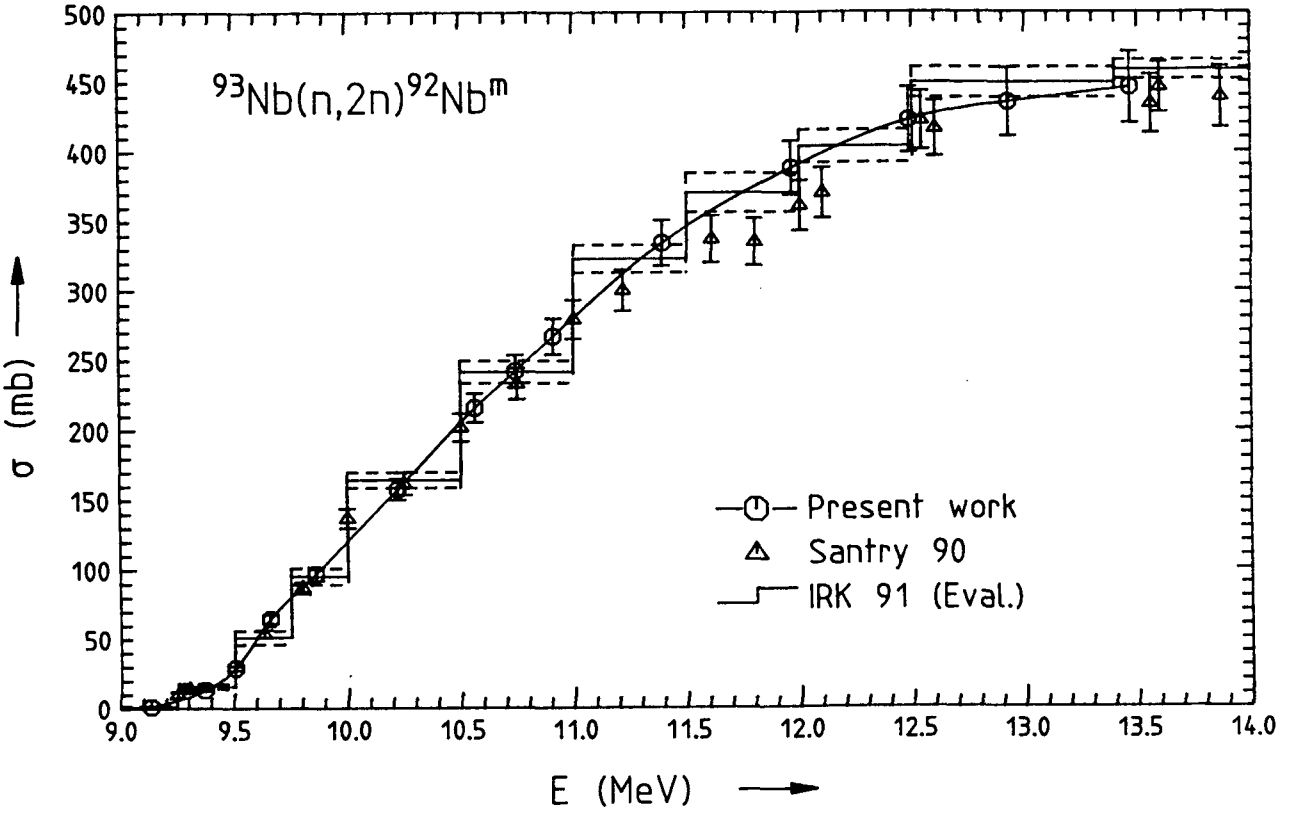

Fig. 2 Cross sections for the $^{93}Nb(n,2n)^{92m}Nb$ reaction. The present data (circles) are interconnected by a smooth curve and compared with the data of Santry and Werner [4]. The step function represents the updated IRK evaluation [5] and the associated uncertainties.

^{238}U fission deposit acting as neutron fluence monitor. Monte Carlo calculations were done to estimate the contribution of scattered neutrons to the reaction rates. Due to the high neutron threshold energy of $^{93}Nb(n,2n)^{92m}Nb$, parasitic neutrons from the D(d,np) breakup reaction contributed only to the ^{238}U fission rates. Appropriate corrections for this were calculated on the basis of detailed experimental data of the breakup reaction. In Fig. 2 the result of the present experiment is shown and compared with another recent experiment [4]. For the sake of completeness, the result of the updated IRK evaluation [5] is also shown. This evaluation comprises data of the present work and those from Ref. [4] and deviates substantially from a previous version based on experiments performed before 1990.

1.3 Activation Cross Sections of ^{105}Ag for Neutron Energies between 20 MeV and 70 MeV

U.J. Schrewe, M. Matzke, R. Nolte, H.J. Brede, H. Schuhmacher

Because of the high threshold energies of 18 MeV and 35 MeV, the activation of ^{105}Ag (half-life: 41 days) by reactions with silver of natural isotopic composition is suitable for a particularly selective detection of neutrons with energies between 20 MeV and 70 MeV. The excitation function of the ^{105}Ag activation had so far been known only up to an energy of 28 MeV [6]. In quasi-monoenergetic neutron fields with energies of up to 70 MeV, as they are available at the Paul Scherrer Institute (PSI), Switzerland, and at the University of Louvain-la-Neuve, the cross sections of the $^{107}Ag(n,3n)^{105}Ag$ and $^{109}Ag(n,5n)^{105}Ag$ reactions were investigated. The spectral neutron fluence, the absolute fluence and the activation measurements were performed at energies of 27, 31, 38, 39, 45, 60, 64 and 66 MeV. The sum of the two activation cross sections σ was determined by measuring the number of the ^{105}Ag atoms per neutron fluence activated in a sample. The large energy range and the background of low-energy neutrons, which cannot be avoided in the production of high-energy neutron fields, presented particular difficulties. It was therefore necessary to also measure the spectral neutron fluence Φ_E, in addition to the absolute neutron fluence Φ, and to determine the desired excitation function $\sigma(E)$ by deconvolution of a linear integral equation. The deconvolution procedures [7] start from a guessed form of the excitation function and vary this function until as small a difference as possible between the calculated and the measured values of σ is obtained. Fig. 3 shows the excitation function of ^{105}Ag determined in this way, and the guess functions which have resulted from a theoretical model calculation [9].

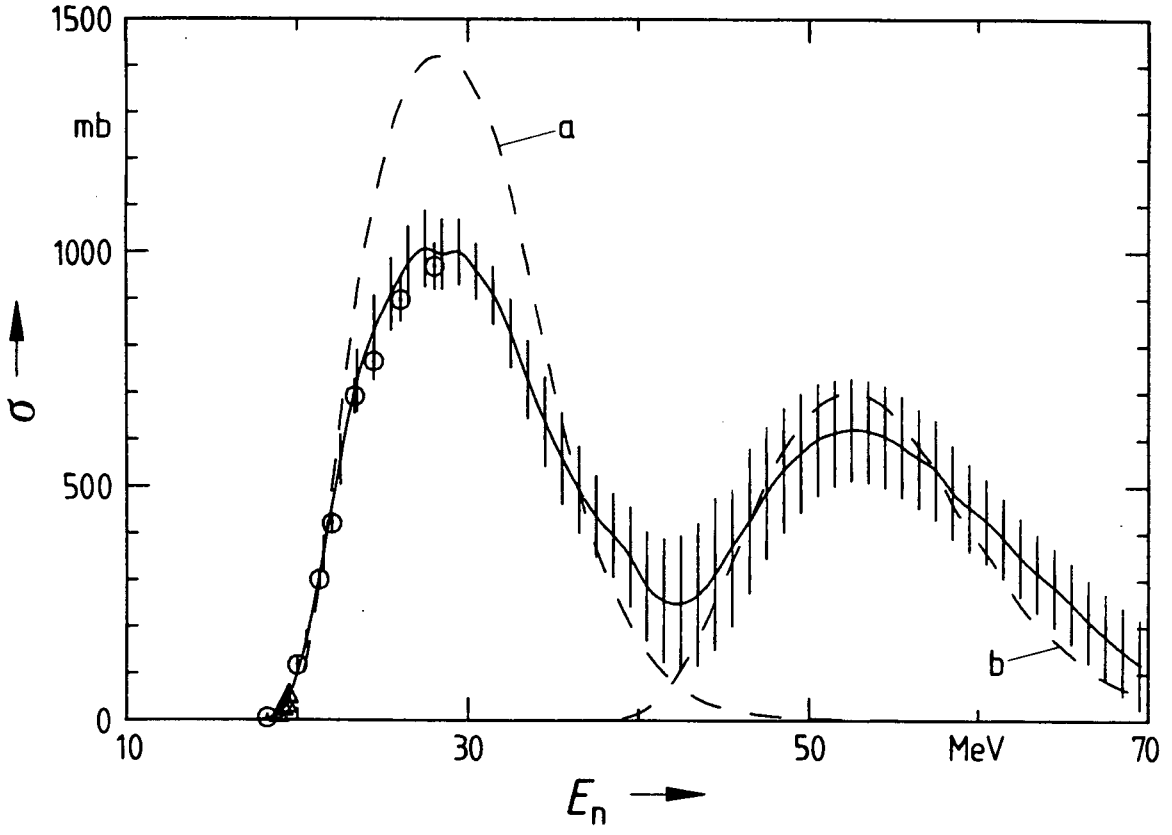

Fig. 3 Activation cross section σ(E) of ^{105}Ag as the result of a deconvolution calculation [7], carried out on the basis of six measurements of mean cross sections σ and spectral neutron fluences Φ_E (solid line). The data points below 28 MeV are experimental values taken from the literature [6,8]. The broken line curves represent the result of a theoretical model calculation [9]; they have been used as initial values of the deconvolution calculation.

1.4 Neutron Scattering from Elemental Iron

D.Schmidt, W.Mannhart, R.Nolte

Neutron scattering from elemental iron has been investigated in the energy range above 10 MeV. In a first step, measurements were done at incident energies of 10.0, 11.0, 11.4, 12.4 and 13.1 MeV, but an extention to energies of up to 15 MeV is intended.

The experimental TOF spectra are compared with iteratively adjusted Monte Carlo calculations. With an additional polyethylene sample the cross sections are normalized to n-p scattering. The averaged magnitude of the multiple scattering correction is in the order of

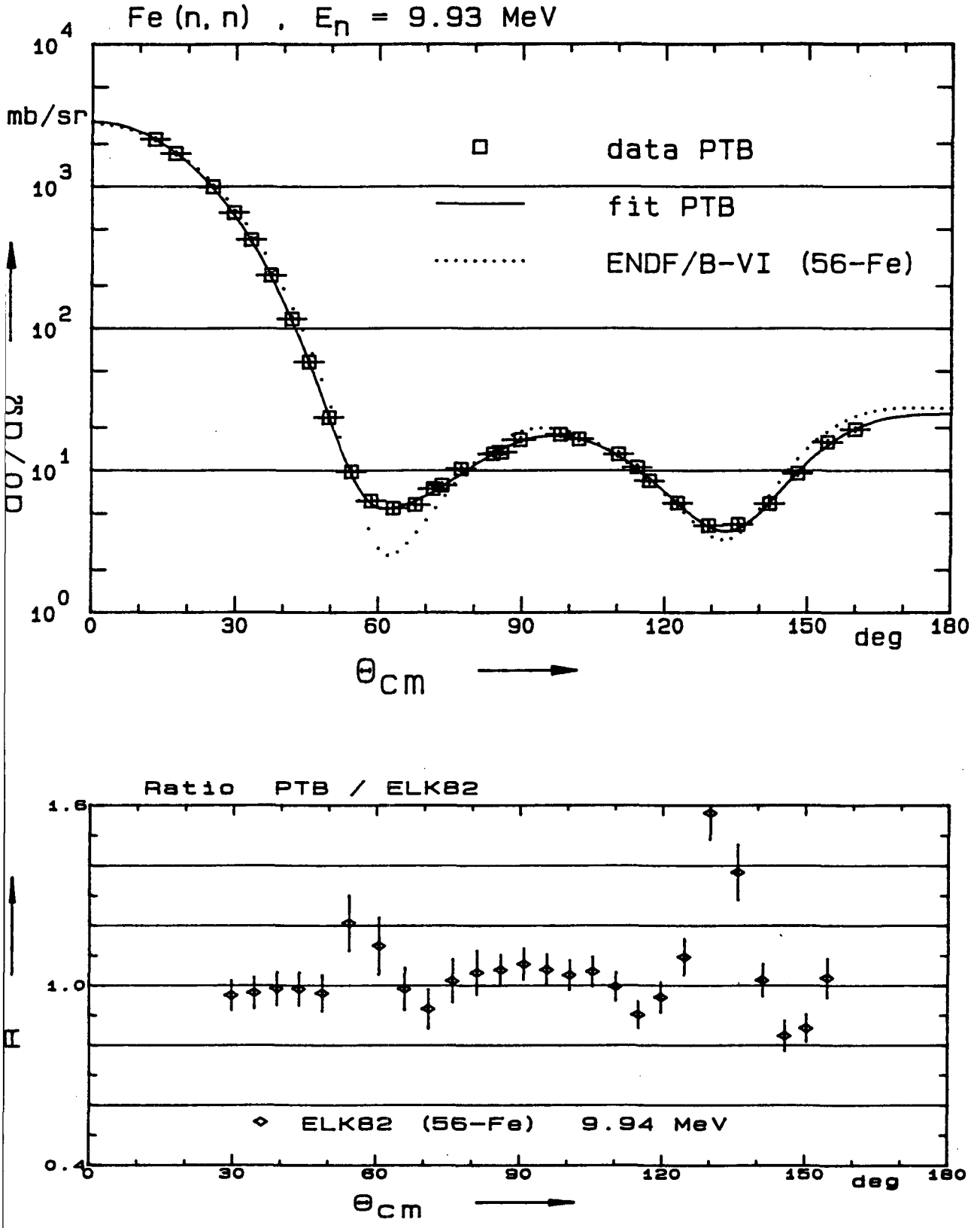

Fig. 4 Elastic angular distribution from elemental iron (upper part), PTB = this work; comparison with other data (lower part), taken from Ref. [10] (= ELK82).

15%, but in particular up to 65% (in the first minimum of the elastic angular distribution at 10 MeV), it depends only weakly on the sample size.

In addition to the elastic scattering, the first excited state in ^{56}Fe (0.847 MeV) was analysed to obtain cross sections. The elastic and inelastic scattering peaks were separated between 3.0 fwhm (10 MeV) and 2.5 fwhm (13 MeV). Thus, the overlap of the elastic and the inelastic peak caused by the unsymmetric peak shape was carefully studied.

As a preliminary result, Fig. 4 shows the elastic angular distribution at 10 MeV in comparison with the ENDF/B-VI evaluation. In the lower part a comparison with data from Ref. [10] is shown. The deviations may be partly due to the use of elemental and isotopic samples.

1.5 Measurement of the $^{12}C(n,\alpha)^{9}Be$ Cross Section via the Inverse Reaction $^{9}Be(\alpha,n)^{12}C$

D. Schmidt, R. Böttger, H.Klein, R. Nolte

The previously reported measurement was extended to a total of 19 alpha energies between 7.02 and 15.70 MeV.

A new target assembly was used which was tilted by about 45 deg. in relation to the beam axis. The attenuation of the outgoing neutrons in the full angular range (0 - 157°) was, therefore, less than 2.5%. During the measurement period, the intensity of satellite pulses caused by the principle of the compact cyclotron could be kept at a portion of less than 3%, resulting in an uncertainty contribution of less than 1%, an exception being only one energy (E_α = 8.49 MeV).

The efficiency curves were needed up to 21 MeV neutron energy. Correction factors were deduced by comparing detector spectra calculated for different energies with experimental ones, measured at lower detection thresholds (nearly 250 keV). Such corrections compensate the fact that the reaction cross sections of the neutron detection processes, e.g. (n,α), (n,p), (n,d), are not known with sufficient accuracy in the energy range below 21 MeV.

The experimental procedure briefly described here is discussed in detail in Ref. [11]. In addition to the $^{9}Be(\alpha,n)^{12}C$(g.s.) cross sections, the cross sections of the $^{9}Be(\alpha,n)^{12}C(E_{ex})$ reaction to the higher-lying states in ^{12}C with E_{ex} = 4.439 MeV to 12.71 MeV were also derived. All these cross sections, including those to the inverse $^{12}C(n,\alpha)^{9}Be$(g.s.) reaction, are given in Ref. [12], together with figures illustrating the quality of the Legendre expansion least-squares fits.

1.6 Test of two Monte Carlo Codes for the Calculation of Scintillation Detector Efficiencies in the Energy Range between 20 and 70 MeV

R. Nolte, H. Schuhmacher, H.J. Brede, U.J. Schrewe

An NE213 detector 5.1 cm in diameter and 10.2 cm in length has been used to measure the spectral fluence distribution in quasi-monoenergetic neutron beams applying the TOF technique. The beams were produced with the ^{9}Be(p,n) reaction for proton energies of 50 and 71.3 MeV. The neutron fluence in the peak region of the spectral distribution has been determined with a proton recoil telescope (PRT) of the Los Alamos design.

The efficiency and the response of the scintillation detector have been calculated with the Monte Carlo codes SCINFUL [13] and KENT01 [14]. Two procedures have been followed to derive the spectral fluence:

For the fixed-threshold technique, TOF spectra acquired for a fixed detection threshold are required. The detector efficiency is calculated for the full response above this threshold, including the contributions from fast neutron reactions with carbon nuclei for which accurate cross sections are lacking. Detector responses falsely predicted as a result of an insufficient description of these channels therefore make themselves felt in a threshold dependence of the derived spectral fluence distribution.

The normalization technique requires the simultaneous measurement of the pulse height and the TOF parameter for each event. Pulse height spectra for almost monoenergetic neutrons are obtained by restricting the TOF parameter to small intervals. The neutron fluence for each TOF interval is determined by normalizing calculated pulse height spectra to the experimental ones. Any ambiguities due to n-C reactions are avoided by restricting the normalization to the high pulse height portion of the response spectra, which is exclusively determined by n-p scattering. The uncertainty of the method depends crucially on the differential n-p scattering cross section at backward angles and on the accuracy of the Monte Carlo modelling, including effects like multiple scattering, incomplete stopping of charged particles and scintillation light losses.

When the n-p cross section data sets used in SCINFUL and KENT01 were checked, considerable deviations from the most recent phase shift analysis ("VL35") of Arndt et al. [15] were found. Since the phase shift results were used to analyse the PRT data, the original SCINFUL cross sections were replaced by this data set in order to achieve consistency between the PRT and the scintillator measurements. No changes were made in the KENT01 code.

Table 1 shows the spectral neutron fluence Φ_p/Q integrated over the peak region (E_n = 38 -50 MeV for E_p = 50 MeV, E_n = 58 MeV - 71 MeV for E_p = 71.3 MeV) and normalized to the beam charge Q. The scintillation detector data have been analysed using the normalization technique with the modified SCINFUL code. The uncertainty does not include the contribution due to the n-p cross section (5% for $\overline{E_n}$ = 44.5 MeV, 6% for $\overline{E_n}$ = 66.0 MeV) which cancels out in the comparison of the PRT and the scintillator results.

Tab. 1: Peak neutron fluence measured with the PRT and the scintillation detector using the normalization method

$\overline{E_n}$	PRT Φ_p/Q	NE213 Φ_p/Q
MeV	$cm^{-2}nC^{-1}$	$cm^{-2}nC^{-1}$
44.5	10.5(5)	10.1(6)
66.0	10.3(5)	10.3(7)

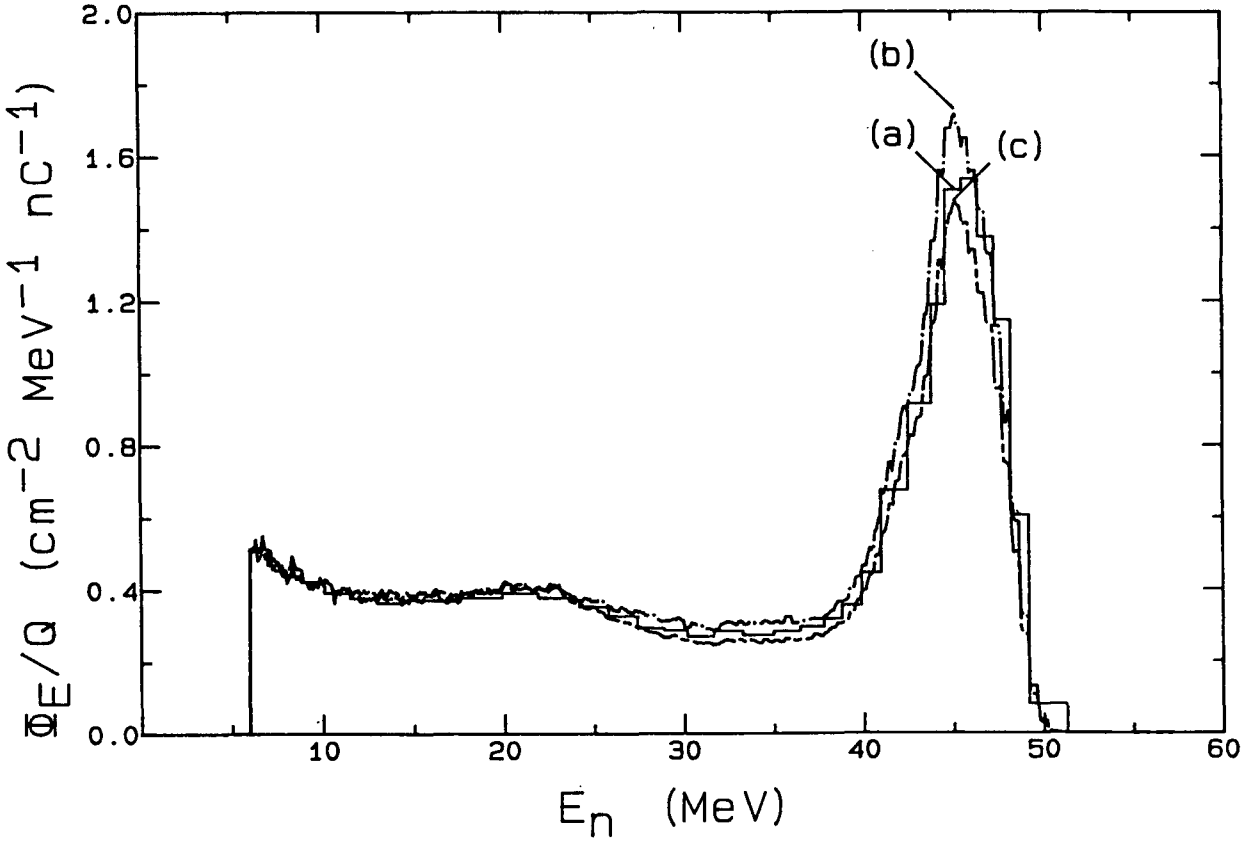

Fig. 5 Spectral neutron fluence for E_p = 50 MeV; (a): normalization technique, modified SCINFUL code; (b): fixed-threshold technique, detector efficiency calculated with the modified SCINFUL code for a threshold of 2 MeV_{ee}; (c): the same as (b) but with the KENT01 code

In contrast to the good agreement obtained with the normalization method, deviations of up to 15%, depending on the detection threshold, were found for the fixed-threshold technique. The spectral fluence distributions obtained with both methods for E_p = 50 MeV are shown in Fig. 5. Details of this comparison will be described in a forthcoming report [16].

1.7 Kerma Factors for A-150 Plastic and Carbon in the Energy Range between 20 MeV and 70 MeV

H.J. Brede, R. Nolte, U.J. Schrewe, H. Schuhmacher

The treatment of malignant tumors with neutrons of energies between 20 MeV and 70 MeV urgently requires a reduction of the uncertainty in the determination of the absorbed dose in tissue if neutron therapy is to reach its full potential.

The conversion of the neutron fluence of the beams into absorbed dose is based on kerma factors [17]. The kerma factors of A-150 plastic material, a tissue substitute, are of great importance since many absorbed dose measuring devices are made of this material. A-150 plastic material, however, differs from tissue in its oxygen and carbon composition, and a correction of the measured quantities is necessary in order to convert the measured dose into the absorbed dose in tissue. This correction is commonly done by using kerma factors of A-150 plastic, carbon and oxygen.

The neutron kerma was measured in the quasi-monoenergetic collimated neutron beam at the Paul Scherrer Institute in Villigen, Switzerland, with low-pressure proportional counters made of A-150 plastic and carbon. The neutron fluence of the beams was determined with a proton recoil telescope.

In Fig. 6 the kerma factors of A-150 and carbon experimentally determined in the energy range between 20 MeV and 70 MeV are compared with other data obtained with models and calculations. In the energy range between 40 MeV and 70 MeV the calculations of Brenner [18] and Wells [19] agreed best with our results.

The work was supported by the Commission of the European Communities (CEC).

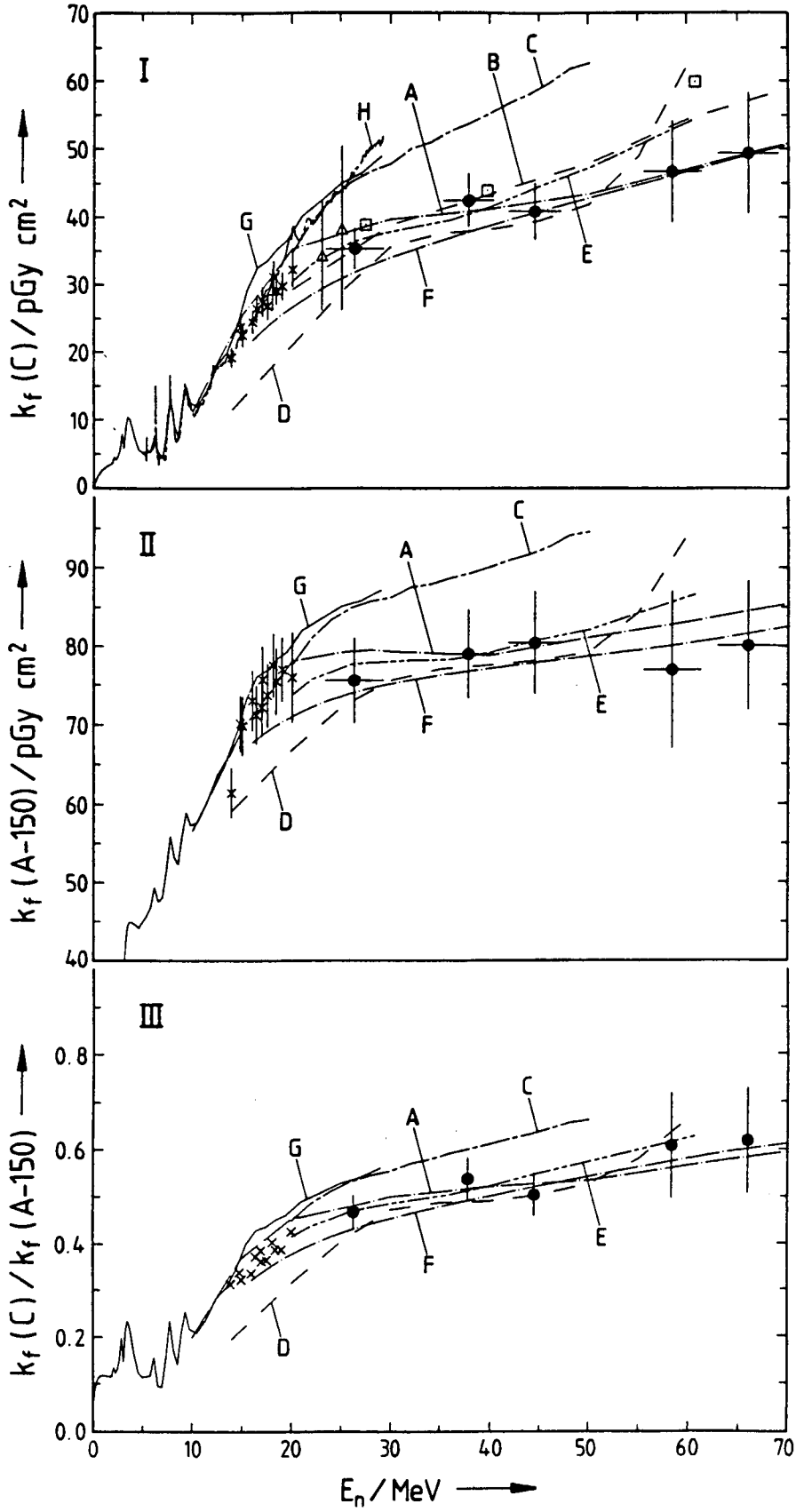

Fig. 6 Kerma factors k_f for carbon, A-150 plastic and the kerma ratio $k_f(C)/k_f(A\text{-}150)$ as a function of the neutron energy E_n. Data points of other authors (A-H), PTB measurements (♦) and evaluations A [19] and F [18].

2. Radionuclide Data

2.1 Half-Lives

H. Schrader

Half-live values were obtained by following the radioactive decay with an ionization chamber. Recently determined results are given in Table 2. Some of them have already been reported elsewhere [20].

2.2 Gamma- and X-Ray Emission Probabilities

U. Schötzig

Gamma- and X-ray emission probabilities per decay of ^{75}Se have been derived from emission rates measured with Ge and Si(Li) detectors, and the activity measured with a 4π-gamma integral counting system. Results have been published [21].

Table 2: Half-live measurements

Nuclide	n	t/T_{12}	$T_{1/2}$	
^{85}Kr	638	1.2	3915(3)	d
^{90}Sr	205	0.15	10513(14)	d
$^{108}Ag^{m}$	233	0.02	418(15)	a
^{133}Ba	787	1.5	3841(5)	d
^{152}Eu	888	1.15	4936(2)	d
^{154}Eu	671	1.5	3139(2)	d
^{186}Re	329	7.3	3.718(1)	d

n: Number of measurements
t: Duration of measurements

References

[1] J.W. Meadows, D.L. Smith, L.R. Greenwood, L.P. Geraldo, W. Mannhart, G. Börker: Proc. Int. Conf. on Nuclear Data for Science and Technology, 13 - 17 May 1991, Jülich, Germany (in press)

[2] T.B. Ryves: European App. Res. Rept. - Nucl. Sci. Technol. 7 (1989) 1241

[3] D.L. Smith, J.W. Meadows, H. Vonach, M. Wagner, R.C. Haight, W. Mannhart: Proc. Int. Conf. on Nuclear Data for Science and Technology, 13 - 17 May 1991, Jülich, Germany (in press)

[4] D.C. Santry, R.D. Werner: Can. J. Phys. 68 (1990) 582

[5] M. Wagner: Report INDC(AUS)-014/L (October 1991)

[6] B.P. Bayhurst et al.: Phys. Rev. C12 (1975) 451

[7] F.G. Perey: Report ORNL/TM-6062 (1977)

[8] H. Liskien: Nucl. Phys. A118 (1968) 379

[9] M. Blann, J. Bisplinghoff: LLNL Report: UCID-19614 (1983), Lawrence Livermore National Laboratory

[10] El-Kadi et al.: Nucl.Phys. A 390 (1982) 509 and EXFOR 10958

[11] D.Schmidt, R.Böttger, H.Klein, R.Nolte: Report PTB-N-7, Physikalisch-Technische Bundesanstalt Braunschweig (1992)

[12] D.Schmidt, R.Böttger, H.Klein, R.Nolte: Report PTB-N-8, Physikalisch-Technische Bundesanstalt Braunschweig (1992)

[13] J.K. Dickens: Report ORNL-6463 (1987)

[14] R.A. Cecil et al.: Nucl. Instr. and Meth. 161 (1979) 439 and
W.C. Sailor et al.: Nucl. Instr. and Meth. A277 (1989) 599

[15] R.A. Arndt et al.: Phys. Rev. D35 (1987) 128 and private communication

[16] R.Nolte et al.: to be published as Report PTB-N-9

[17] ICRU Report 33: International Commission on Radiation Units and Measurements, Washington, D.C. (1980)

[18] D.J. Brenner: Phys. Med. Biol. 29 (1983) 437

[19] A.H. Wells: Radiat. Res. 80 (1979) 1

[20] U. Schötzig, H. Schrader, K. Debertin: Proc. Int. Conf. on Nuclear Data for Science and Technology, 13 - 17 May 1991, Jülich, Germany (in press)

[21] U. Schötzig: Nucl. Instr. and Meth. A312 (1992) 141

FACHINFORMATIONSZENTRUM KARLSRUHE

STATUS REPORT

H. Behrens, H.-W. Müller

1. Information Systems with Relevance to Nuclear Data

a) The Physics Database (PHYS)

This database covers the worldwide appearing literature on physics, astronomy and related topics since 1979. It appears in printed form as "Physics Briefs" derived from "Physikalische Berichte", an abstracting journal founded in 1845. There is also a good coverage of Eastern European and East Asian literature. Data sources were in 1991:

- journals (83%)
- books (14%)
- reports (1.7%)
- other non-conventional literature (1.2%)
- conference contributions (29%)

Traditionally, nuclear physics is a major part of the physics database. The numbers of citated nuclear relevant articles are (Apr. 92):

458	Nuclear physics (general)
28,425	Nuclear structure
12,305	Radioactivity and electromagnetic transitions
12,301	Nuclear reactions and scattering (general)
53,082	Nuclear reactions and scattering (specific reactions)
7,270	Nuclear engineering and nuclear power studies
51,442	Experimental methods and instrumentation for elementary-particle and nuclear physics

The database is updated 24 times annually. PHYS is available online from the Scientific and Technical Information Network (STN). Access is possible via DATEX-P or WIN nets, or, on request, from FIZ KARLSRUHE.

b) Evaluated Nuclear Structure and Decay Data File (ENSDF)

Nuclear Structure and Decay Data are evaluated by the International Network of Nuclear Structure and Decay Evaluators and published as the well-known Nuclear Data Sheets or in the Nuclear Physics journal. Data are available as of version ENSDF-020 (Sep 91). The file covers 11,245 datasets, each representing a special type of nuclear physics experiment. In total it comprises 1,028,238 data records, each of 80 bytes length. Data can be obtained on request from the FIZ KARLSRUHE.

c) Catalog of Gamma Rays and Alpha Particles from Radioactive Decay (GAMCAT)

GAMCAT is a Personal Computer database system comprising 46,950 gamma and 1,904 alpha lines, originating from more than 2,200 radionuclides. It is designed for use in gamma and alpha spectrometry as well as in cross-section measurements, activation analysis, environmental pollution control or waste composition control . GAMCAT runs on an AT-compatible computer with hard disk and 640 K of memory, operating under DOS 2.11 or later. 2 M of storage are needed on the hard disk. It is distributed on two HD floppy disks.

d) Inorganic Crystal Structure Data File (ICSD)

ICSD is a comprehensive compilation of data defining crystal structure of inorganic compounds, based preferentially on X-ray and neutron diffraction studies. It includes the crystal parameters like unit cell, space group, atomic coordinates, thermal parameters etc. and, additionally, experimental methods and bibliographic data. Both investigations of powders and single crystals are covered. Hence ICSD is a useful tool to obtain information about neutron diffraction on inorganic materials.

Data are critically evaluated from journal articles. Presently (Apr. 92), ICSD covers about 33,000 entries. The file is updated twice a year.

ICSD is produced by FIZ KARLSRUHE and the GMELIN Institute, Frankfurt, in cooperation with the Institute of Inorganic Chemistry of the University Bonn. It can be retrieved online from the STN Host. In-house and CD-ROM versions are also available.

2. Data Compilations

A further issue with nuclear data appeared in our series PHYSICS DATA:

> Evaluation of 14 MeV Cross Sections for the Main Isotopes of the Structural Materials Cr, Fe and Ni
> A. Pavlik, S.Tagesen, H. Vonach, M. Wagner
> PHYSICS DATA 13-6 (1991)

APPENDIX

Addresses of Contributing Laboratories

Institut für Kernphysik III
Director: Prof. Dr. G. Schatz
Senior reporter: Dr. F. Käppeler
Kernforschungszentrum Karlsruhe
Postfach 3640
W-7500 Karlsruhe

Institut für Materialforschung I
Director: Prof. Dr. K.-H. Zum Gahr
Senior reporter: Dr. S. Cierjacks
Kernforschungszentrum Karlsruhe
Postfach 3640
W-7500 Karlsruhe

Institut für Neutronenphysik und Reaktortechnik
Director: Prof. Dr. G. Kessler
Senior reporter: Dr. F. Fröhner
Kernforschungszentrum Karlsruhe
Postfach 3640
W-7500 Karlsruhe

Institut für Kernphysik,
Arbeitsgruppe Strahlungstransport
Head and senior reporter: Dr. D. Filges
Forschungszentrum Jülich
Postfach 1913
W-5170 Jülich

Institut für Nuklearchemie
Director: Prof. Dr. G. Stöcklin
Senior reporter: Dr. S.M. Qaim
Forschungszentrum Jülich
Postfach 1913
W-5170 Jülich

Institut für Sicherheitsforschung
Acting director: Dr. F.P. Weiß
Senior reporter: Dr. K. Dietze
Forschungszentrum Rossendorf
Postfach 19
O-8051 Dresden

Institut für Kern- und Atomphysik
Acting director: Prof. Dr. K. Seidel
Technische Universität Dresden
Außenstelle Pirna-Copitz
Pratzschwitzer Str. 15
O-8300 Pirna

Zentraleinrichtung für Strahlenschutz
Head and senior reporter: Prof. Dr. H. Michel
Universität Hannover
Am Kleinen Felde 30
W-3000 Hannover 1

Abteilung Nuklearchemie
Director: Prof. Dr. G. Stöcklin
Senior reporter: Dr. U. Herpers
Universität zu Köln
Zülpicher Str. 47
W-5000 Köln 1

Fachbereich Physikalische Chemie
Kernchemie
Senior reporter: Prof. Dr. P. Patzelt
Phillipps-Universität Marburg
Lahnberge
W-3550 Marburg/Lahn

Physikalisch-Technische Bundesanstalt
Abteilung 6, Atomphysik
Director: Prof. Dr. R. Jahr
Bundesallee 100
W-3300 Braunschweig

Fachinformationszentrum Energie, Physik, Mathematik
Directors: Dr. W. Rittberger, E.-O. Schulze
Senior reporters: Dr. H. Behrens, Dr. H.-W. Müller
Kernforschungszentrum
W-7514 Eggenstein-Leopoldshafen